

Dear Oliver Bothe,

Thanks for your positive comments and suggestions. Please, find our answers below.

General comments

There is one suggestion for the future of the database. I would like to invite the authors to reconsider the general structure of the database and/or to provide a set of functions that allow an even easier interaction with the data than is already the case. Obviously, it is unlikely that there is a set of tools that accounts for all preferences of all potential users, and neither is it likely that there is a database structure that is intuitive even for the most inexperienced user. This suggestion originates from my struggles to access the data.

Accessing and querying any database is challenging for non-specialists but, as the reviewer acknowledges, it would be impossible to provide functions for all types of software and that addresses all the preferences that data users may have. To facilitate potential database users, we have created a set of “example queries” that are available along with the database files. While these 27 queries do not cover all potential needs of the researchers using the database, they provide a starting point. The existence of the example queries is mentioned in the README file available with the database in the data repository, but we will add text in the manuscript to make this clearer.

The structure of the database was agreed with the wider speleothem community as the most efficient way to capture the metadata and data available from speleothem records. A detailed description of the database and all its parameters is available in the paper describing the first version of the database (Atsawaranunt et al., 2018). We will make sure that this is clear in the text. Note that it is also possible to download the individual tables comprising the database, allowing a user to reconfigure this in any format they prefer.

Minor

Suggestion: Add a list of abbreviations and technical terms. From my point of view, a database and a database paper is of interest for a community that extends beyond the specialists in a field. Therefore it might be advisable to provide a table or an appendix with definitions of technical terms and abbreviations. Otherwise, already Figure 1 may overwhelm some potential users.

In this paper, we did not define all concepts presented in the current database structure because these are already defined in Atsawawaranunt et al., 2018. This publication is cited in the manuscript as the source to look at for a detailed description of the database (L170-172: “*The structure and contents of all tables except the new sisal_chronology table are described in detail in Atsawawaranunt et al. (2018a). Here, we focus on the new sisal_chronology table and on the changes that were made to other tables in order to accommodate this new table (See section 2.3).*”).

We are unsure as to whether providing that information again in the supplementary material of this paper would make things substantially different than referring to a paper previously published in the same journal. However, we will make it clear earlier in the manuscript that all concepts that appear in the database are defined in that publication and we hope that this will address the reviewer’s concern satisfactorily.

Line 16: The authors write here 294 and later 293. Obviously “cave sites” and “cave systems” may mean different things, but I would like to ask the authors to clarify.

We used cave sites and cave systems interchangeably but will change it to cave sites throughout.

Line 81: 10.5281/zenodo.3591197 is not a valid doi, i.e. the link is broken.

Thank you for spotting this. The link to the ensemble file is now working.

This occurs again at line 271.

Thank you for spotting this. This link is now working properly.

The doi in line 270 is not valid either.

Thank you for spotting this. This link is now working properly.

Finally, in section 6 (lines 273,274, 276) and in the supplementary materials there are a few dois given as links but missing the “doi.org”-part and therefore not working directly.

Thanks. We will revise the hyperlinks in the manuscript as well as in the supplementary material before submitting a revised version of this manuscript.

Line 96: “This is consistent” implies that there are differences to these previous approaches. If these differences can be summarised shortly, it may be helpful to detail them.

By “this is consistent” we mean that our approach is equivalent, in that it produces highly similar results (apart from small numerical differences

we expect due to the choice of random number generator and interpolation depths as well as, for COPRA the different programming language). We will clarify this in the revised document.

Provide a script to reproduce Figure 5. I would like to suggest to provide a script that reproduces Figure 5. Parts of this are already included in the GitHub repository for SISAL.AM, cf. the `plot_sisal_overview.R` script. However, the `final.plot` function is only partially doing this and the script does not run as it is. The reading of the input-files has two errors (that can be easily corrected).

We have updated the GitHub repository for SISAL.AM with a script to successfully produce figure 5 as requested by the reviewer: https://github.com/paleovar/SISAL.AM/tree/master/SISAL_plot_functions

Technicalities

Some of the following technicalities are purely subjective. Some are meant to capture already at this stage some of the annotations that will come because of Copernicus' copy editing efforts.

Line 22: Please rephrase the sentence in combination with the parentheses. I am also unsure whether the tense of the verb in the parentheses is correct.

We will rephrase this sentence to: “Speleothems are a rich terrestrial palaeoclimate archive that forms from infiltrating rainwater after it percolates through the soil, epikarst, and carbonate bedrock.”

Line 23: I stumbled between the first and second sentence of the paragraph as I felt they were rather badly connected. But that is rather subjective.

We agree with this comment and we will revise these two sentences to: “Speleothems are a rich terrestrial palaeoclimate archive that forms from infiltrating rainwater after it percolates through the soil, epikarst, and carbonate bedrock. In particular, stable oxygen and carbon isotope ($\delta^{18}\text{O}$, $\delta^{13}\text{C}$) measurements made on speleothems have been widely used to reconstruct regional and local hydroclimate changes.”

Line 25: Again subjectively, I felt there should already be a new paragraph here.

We agree with the reviewer and we will move the sentence starting with “The Speleothem Isotope Synthesis. . .” to a new paragraph.

Line 40: I assume it should read “pointed to the” instead of “pointed the”.

We agree and we will apply this change.

Line 48: The authors use two different notations for COPRA; COPRA and copRa. It may be that copRa is meant only to refer to the implementation of COPRA, but that does not become clear. I invite the authors to either only use one notation or to clearly specify that copRa is COPRA for R. In this context, I also would invite the authors of copRa to make copRa publically available. Giving an official acronym to the author's COPRA implementation in R already suggests such an availability.

Indeed, copRa is the R implementation of COPRA created specifically for this paper. We will revise the text to make this clear.

As stated in the data availability section, this new copRa implementation is already publicly available at <https://github.com/paleovar/SISAL.AM>.

Similarly it would be nice, if the authors' updated version of StalAge could be made available. This may be already the case, then I missed the pointer. It may be that all what I am writing here is already fulfilled by Roesch (2020, <https://github.com/paleovar/SISAL.AM>). If that is the case then please put the link at all positions where it is relevant.

Yes, as stated in the data availability section, the modified version of StalAge is already publicly available at <https://github.com/paleovar/SISAL.AM>. We will add the links were appropriate in addition to the "data availability section" to make this clear.

Oh, and the link to github.com/palaeovar/SISAL.AM given by the authors does not work.

Apologies, the correct link is <https://github.com/paleovar/SISAL.AM> (without the "a" of palaeo). We will correct the link in the manuscript.

Line 154: The authors mention the function *pchip* but not the package. I ask them to add the package and a citation for it. There may be other instances where this is necessary.

The *pchip* function comes from the signal R package, we will add this in the reference list.

We will provide the package name and a citation for it every time that an R function is mentioned in the manuscript.

Personal communications: If I remember correctly, Copernicus' editors are asking authors to provide the year of personal communication and also full names.

We will revise this to: “(Christoph Bronk Ramsey, personal communication, 2019).”

Similarly, the copy editors/typesetting editors are going to check for completeness of citations. I think I noted some missing information, e.g., the DOI for Rehfeld and Kurths (2014). Maybe the authors want to check all citations for completeness already at this stage.

Thanks for spotting this. We will revise all DOIs and references before submitting a revised version of the manuscript.

All links: please provide last accessed dates for all URLs.

We will do.

R packages: I did not check in detail - and I do not always follow this idea myself - but I think it would be nice if the authors could not only mention the R packages they use but also provide references for each of them. It may be that they already do this. I only noted that, e.g., for rBacon there is not a direct reference given, but maybe this is already fulfilled with the references in line 124. Another example is the mentioning of Hmisc on line 99.

We will make sure that all R packages that we used are cited were appropriate and that links are always copied where relevant.

There is an R package with rBacon. We mention it in the data availability section: “rBacon package (version 2.3.9.1) is available on CRAN (<https://cran.r-project.org/web/packages/rbacon/index.html>).” but we will also add its citation where appropriate in the text.

We will also cite the packages of Hmisc (L99) and pchip (L154) in the manuscript.

Software in general: The last comment, obviously, also applies to all other sorts of software, e.g., github-links in the manuscript. Similarly, the authors probably should also provide references for the zenodo-dois in the manuscript.

We will double check that all links are properly working before submitting a revised version of the manuscript. We will also properly cite the zenodo-dois mentioned in the manuscript.

Dear Jud W. Partin,

Thanks for your comments and suggestions. Indeed, data compilations are an enormous community-based effort that we believe will have a strong impact on how science is done. Please, find our answers below highlighted in blue.

Can you please describe in more detail how the 95% confidence intervals are calculated (line 227) in the SISAL chronologies? I'm not sure, but I think it is the 95% spread in the ages using all of the age models, i.e. the spread in the curves in Figure 5 a and b. If so, I wholeheartedly support this idea. If not, then please describe in more detail.

The 95% confidence intervals are the spread for each type of age model separately not the spread considering all of the age models. Specifically, the SISAL chronology table has three columns per age-depth model technique. The first is the median age-depth model and the other two are their corresponding 2 sigma confidence intervals. These confidence intervals have been calculated from the spread of the individual ensembles for each technique that support this approach (specifically, linear interpolation, linear regression, Bchron, Bacon, OxCal and copRa)) and the last 1000 have been kept – and made available – for further analyses. For StalAge we report the uncertainties of the returned age model which are internally calculated and based on iterative fits as well as dating uncertainty. Fig. 5a and 5b show the median age models for each technique (the mean for StalAge). Each of these lines has corresponding confidence intervals which are individually reported.

We have not attempted to merge all SISAL chronologies for any given entity. Different modelling approaches give stronger weighting to some age determinations, so averaging across several methods could yield age-depth relationships that are unrealistic and/or not robust compared to the available U-Th dates.

We will add a statement on how the uncertainties are obtained in the description of each age-depth model technique in section 2.1.

Lines 204-210 are hard to follow. (Author's comment: Please note that we have separated this comment from the paragraph above as it refers to different things).

Original text in L204-210 copied for reference: “The conception and the test of the R workflow, integrating all methods but OxCal, was outlined in Roesch and Rehfeld (2019) and includes automatized checks for the final chronologies except for OxCal. The quality control parameters obtained from OxCal were compared with the recommended values of Agreement Index (A) larger than 60 % and Convergence (C) larger than 95 %, in accordance with the guidelines in Bronk Ramsey (2008). In addition to both model agreement and P-Sequence convergence meeting these criteria, at least 90 % of individual dates had to have an acceptable Agreement and Convergence themselves. OxCal age-depth models failing to meet these criteria were not included in the SISAL chronology table.”

We acknowledge that this paragraph needs rewriting and we will add the following text instead:

“We used an automated approach to age-depth modelling in R because of the large number of records. Roesch and Rehfeld (2019) have described the basic workflow concept and tested it using all of the age-modelling approaches used here except OxCal. The basic workflow involves step-by-step inspection and formatting of the data for the different methods, and the use of pre-defined parameter choices specific to each method. Each age-modelling method is called sequentially. An error message is recorded in the log file if a particular age-modelling method fails, and the algorithm then progresses to the next method. If output is produced for a particular age-modelling method, these age models are checked for monotonicity. Finally, the output standardization routine writes out, for each entity and age-modelling approach, the median age model, the ensembles (if applicable) and information of which hiatuses and dates were used in the construction of the age models. These outputs are then added to the sisal-chronology table (Table 2). All functions are available at <https://github.com/paleovar/SISAL.AM> (last access: 23 July 2020) and CRAN (<https://cran.r-project.org/web/packages/rbacon/index.html>; last access: 31 January 2020).

The general approach for the OxCal age models was similar, and step-by-step details and scripts are provided in <https://doi.org/10.5281/zenodo.3586280> (Amirnezhad-Mozhdehi and Comas-Bru, 2019). The quality control parameters obtained from OxCal were compared with the recommended values of Agreement Index (A) larger than 60% and Convergence (C) larger than 95%, in accordance with the guidelines in Bronk Ramsey (2008), both for the overall model and for at least 90% of the individual dates. OxCal age-depth models failing to meet these criteria were not included in the sisal-chronology table (Table 2).”

We agree that the spread of the median age models is useful. However, we do not think it is useful to calculate cross-model uncertainties based on the medians/ensembles of all age models. As explained above, in many cases the resulting merged chronology would not be consistent with the available U-Th dates. However, we supply all the data (medians, uncertainties, ensembles) so that this could be done by individual researchers on an entity by entity basis. Medians and uncertainties are available in the database and ensembles are stored in zenodo: <http://doi.org/10.5281/zenodo.3816804> (Rehfeld et al., 2020).

Our approach does not penalize records with many dates. Usually, the better the spread in dates along a speleothem sample, the more constrained the age-depth model, and the lower the final uncertainty of the best-estimate median age model. However, it should be noted that this is not the case when there is a large number of conflicting U-Th dates with high analytical and correction uncertainties as the resulting age-depth model realisations will substantially differ amongst them.

For example, in Figure 5, there are a string of ages from 3400 – 3550 year BP that all follow each other. For this region of the d18O curve, there is fairly good agreement between the various age modeling techniques. Therefore, when all of those ages are viewed together, our confidence in the timing of any d18O excursion is less than that based on the error bars on each individual date (seen by less 'blur' in Figure 5c between the alternate age models). In other words, the multiple ages help to decrease our uncertainty to less than that of the analytical error bars on each U-Th dates. It's a bit like decreasing the signal to noise ratio by taking more measurements (by the square root of N). (Again SISAL may be doing this, but I'm not sure)

We agree with the reviewer that taking into account multiple chronologies for a given record provides more insights into the age-depth relationship. However, given that all the age models are consistent with the available dates, none of the individual chronologies should be discarded by default. Merging the chronologies obtained using different techniques to obtain "master chronologies for all the SISAL records would lead to a bias towards certain age-modelling approaches. For example, age models created using linear interpolation (successful 403 times) or Bchron (successful 420 times) would usually have a larger weight in a master chronology than Oxcal (successful 106 times) or linear regression (successful 182 times). Unless there is other information that suggests one age model type is better than others for a specific entity, all the chronologies should be considered equally likely.

To quantify the degree to which multiple age modeling techniques may reduce temporal uncertainty, I recommend that this manuscript includes a plot of the average of the analytical error in a record versus the average SISAL 95% chronology error in a record (i.e. average of 5b). Is the fit to that scatter plot a 1:1 line? Or is there a systematic reduction in the error across many records in the database b/c of time periods like 3400-3550 BP in Figure 5? Or do problematic areas, like unresolved hiatuses, compensate the reduction in errors for when the age model is tightly constrained? This would be an enlightening plot.

We do not expect a systematic reduction of the error as a result of the age-depth model techniques used and the data shows that the SISAL uncertainties ultimately depend on the uncertainties of the original U-Th dates and their spread/consistency. In any case, however, this would depend on the robustness of the approach used to treat the uncertainties in each age-depth model.

As suggested by the reviewer, we will add a plot of the average analytical error per record vs the average SISAL chronology uncertainty as attached. The accompanying text will be:

“The published age-depth models of all speleothems are accessible in the original-chronology metadata table and our standardised age-depth models are available at the sisal-chronology table for 512 speleothems. Temporal uncertainties are now provided for 79% of the records in the SISAL database. This is a significantly larger number than in SISALv1b, where most age-depth models lacked temporal uncertainties. Most speleothem records show average U-Th age errors between 100-1,000 years (Figure 6), which are only slightly changed by using age-depth modelling software. Nevertheless, when comparing the mean uncertainties of the U-Th ages with those of their corresponding age-depth model, the slope between both parameters is smaller than one. This indicates that age-depth models tend to reduce uncertainties especially when dating errors are large while they increase uncertainties, when U-Th age errors are small.”

Please give more detail in the text of the principles used in your calculations for when the SISAL chronology decides that there is a hiatus in the record. While you reference Breitenbach, 2012, it would be good to review the guiding principles that SISAL is using in lines 83-86 in more detail to make the manuscript more self contained. Also, what happens if there is disagreement

among the various techniques about a hiatus – how does SISAL decide on a ‘yes’ or ‘no’ to split the record? Does majority rule??

Our age-depth model calculations use the U-Th dates and the depths of the hiatuses as entered in the database and which were provided by the researchers that produced the raw data and/or their publications.

We do not decide in our workflow whether there is (or should be) a hiatus in a section and therefore, all AM approaches use the same input data. For clarity, the input variables for the sisal chronologies are: depths of dating samples and isotopes, U-Th corrected ages and their uncertainties (if used to create the original or published age model), depth information of hiatuses if applicable, information on whether the speleothem was actively growing when collected and the year of collection. We did not attempt to assess whether the information provided by the data contributors/publications was correct. However, together with experts from the SISAL age modelling group we have checked whether the dates and hiatuses were visually consistent with the rest of the data.

We believe there is a misunderstanding as lines 83-86 refer to age reversals that occurred during the construction of the sisal chronologies instead of hiatuses:

“Major challenges arise through hiatuses (growth interruptions) and age reversals. In the classification of the reversals, we distinguish between tractable reversals (with overlapping confidence intervals) and non-tractable reversals (i.e., where the two-sigma-dating uncertainties do not overlap) following the definition of Breitenbach et al. (2012).”

We will rephrase this paragraph to clarify this point:

“Major challenges arise through hiatuses (growth interruptions) and age reversals. We developed a workflow to deal with records with known hiatuses that allowed the construction of age-depth models for 20% of the records with one or more hiatuses (Roesch and Rehfeld, 2019; details below for each age-depth modelling technique). Regarding the age reversals, we distinguish between tractable reversals (with overlapping confidence intervals) and non-tractable reversals (i.e., where the two-sigma-dating uncertainties do not overlap) following the definition of Breitenbach et al. (2012). Details such as the hiatus treatment and outlier age modification are recorded in a logfile created when running the age models. We followed the original author’s choices regarding date usage. If an age was marked as “not used” or “usage unknown”, we did not consider this in the construction of the new

chronologies except in OxCal, where dates with "usage unknown" were considered."

Details on how each technique tackled the hiatuses are copied below (with their corresponding line numbers):

Linear Interpolation: "Hiatuses are modelled following the approach of Roesch and Rehfeld (2019), where rather than modelling each segment separately, synthetic ages with uncertainties spanning the entire hiatus duration are introduced for use in age-depth model construction. These synthetic ages are removed after age-depth model construction. " (lines 100-104)

Linear Regression: "If hiatuses are present, the segments in-between were split at the depth of the hiatus without an artificial age. " (lines 110-111)

Bchron: "Since Bchron cannot handle hiatuses, we implemented a new workflow that adds synthetic ages with uncertainties spanning the entire hiatus duration (Roesch and Rehfeld, 2019), as performed with linear interpolation, StalAge and our implementation of COPRA. " (lines 116-118)

Bacon: "The R package rBacon can handle both outliers and hiatuses and apart from giving the median age-depth model, (...)." (lines 125-126)

Oxcal: "OxCal can deal with hiatuses and outliers and accounts for the non-uniform nature of the deposition process (Poisson process using the P-Sequence command). " (lines 134-136)

COPRA: " (...) we implemented a new workflow in R that adds artificial dates at the location of the hiatuses and prevents the creation of age reversals (Roesch and Rehfeld, 2019) as done with linear interpolation, StalAge and Bchron. " (lines 150-152)

StalAge: "The StalAge v1.0 R function has been updated to R version 3.4 and the default outlier and reversal checks were enabled to run automatically. Hiatuses cannot be entered in StalAge v1.0, but the updated version incorporates a treatment of hiatuses based on the creation of temporary synthetic ages following Roesch and Rehfeld (2019). " (lines 160-163)

SISALv2: A comprehensive speleothem isotope database with multiple age-depth models

Laia Comas-Bru 1, Kira Rehfeld 2, Carla Roesch 2, Sahar Amirnezhad-Mozhdehi 3, Sandy P. Harrison 1, Kamolphat Atsawawaranunt 1, Syed Masood Ahmad 4, Yassine Ait Brahim 5, Andy Baker 6, Matthew Bosomworth 1, Sebastian F.M. Breitenbach 7, Yuval Burstyn 8, Andrea Columbu 9, Michael Deininger 10, Attila Demény 11, Bronwyn Dixon [1,12](#), Jens Fohlmeister 13, István Gábor Hatvani 11, Jun Hu 14, Nikita Kaushal 15, Zoltán Kern 11, Inga Labuhn 16, Franziska A. Lechleitner 17, Andrew Lorrey 18, Belen Martrat 19, Valdir Felipe Novello 20, Jessica Oster 21, Carlos Pérez-Mejías 5, Denis Scholz 10, Nick Scropton 22, Nitesh Sinha 23, [24](#) Brittany Marie Ward [2425](#), Sophie Warken [2526](#), Haiwei Zhang 5 and SISAL Working Group members*.

Correspondence: Laia Comas-Bru (l.comasbru@reading.ac.uk)

Affiliations:

- 1 School of Archaeology, Geography, and Environmental Science, University of Reading, UK
- 2 Institute of Environmental Physics and Interdisciplinary Center for Scientific Computing, Heidelberg University, Germany
- 3 School of Geography. University College Dublin. Belfield, Dublin 4, Ireland
- 4 Department of Geography, Faculty of Natural Sciences, Jamia Millia Islamia, New Delhi, India
- 5 Institute of Global Environmental Change, Xi'an Jiaotong University, Xi'an, Shaanxi, China
- 6 Connected Waters Initiative Research Centre, UNSW Sydney, Sydney, New South Wales 2052, Australia
- 7 Department of Geography and Environmental Sciences, Northumbria University, Newcastle upon Tyne, UK
- 8 The Fredy & Nadine Herrmann Institute Earth Sciences, The Hebrew University of Jerusalem, The Edmond J. Safra Campus, Jerusalem 9190401, Israel
- 9 Department of Biological, Geological and Environmental Sciences (BiGeA), University of Bologna, Via Zamboni 67, 40126, Bologna, Italy
- 10 Institute for Geosciences, Johannes Gutenberg University Mainz, J.-J.-Becher-Weg 21, 55128 Mainz, Germany
- 11 Institute for Geological and Geochemical Research, Research Centre for Astronomy and Earth Sciences, H-1112, Budaörsi út 45, Budapest, Hungary
- 12 School of Geography, University of Melbourne, Australia; ~~School of Archaeology, Geography, and Environmental Science, University of Reading, UK~~
- 13 Potsdam Institute for Climate Impact Research PIK, Potsdam, Germany
- 14 Department of Earth, Environmental and Planetary Sciences, Rice University, US
- 15 Asian School of the Environment, Nanyang Technological University, Singapore
- 16 Institute of Geography, University of Bremen, Celsiusstraße 2, 28359 Bremen, Germany
- 17 Department of Earth Sciences, South Parks Road, Oxford OX1 3AN, UK
- 18 National Institute of Water and Atmospheric Research, Auckland, 1010, New Zealand
- 19 Department of Environmental Chemistry, Spanish Council for Scientific Research (CSIC), Institute of Environmental Assessment and Water Research (IDAEA), Barcelona, Spain
- 20 Institute of Geoscience, University of São Paulo
- 21 Department of Earth and Environmental Sciences, Vanderbilt University, Nashville, TN 37240, US

22 School of Earth Sciences, University College Dublin, Belfield, Dublin 4, Ireland

23 ~~IBS~~-Center for Climate Physics (~~ICCP~~), Institute for Basic Science, Busan, Republic of Korea, 46241

24 Pusan National University, South Busan, Republic of Korea, 46241

2425 Environmental Research Institute, University of Waikato, Hamilton, New Zealand

2526 Institute of Earth Sciences and Institute of Environmental Physics, Heidelberg University, Germany

* A full list of authors appears at the end of the paper.

1 **Abstract:**

2 Characterising the temporal uncertainty in palaeoclimate records is crucial for analysing past climate
3 change, for correlating climate events between records, for assessing climate periodicities, identifying
4 potential triggers, and to evaluate climate model simulations. The first global compilation of speleothem
5 isotope records by the SISAL (Speleothem Isotope Synthesis and Analysis) Working Group showed that
6 age-model uncertainties are not systematically reported in the published literature and these are only
7 available for a limited number of records (ca. 15%, $n = 107/691$). To improve the usefulness of the SISAL
8 database, we have (i) improved the database's spatio-temporal coverage and (ii) created new
9 chronologies using seven different approaches for age-depth modelling. We have applied these
10 alternative chronologies to the records from the first version of the SISAL database (SISALv1) and to new
11 records compiled since the release of SISALv1. This paper documents the necessary changes in the
12 structure of the SISAL database to accommodate the inclusion of the new age-models and their
13 uncertainties as well as the expansion of the database to include new records and the quality-control
14 measures applied. This paper also documents the age-depth model approaches used to calculate the new
15 chronologies. The updated version of the SISAL database (SISALv2) contains isotopic data from 691
16 speleothem records from 294 cave sites and new age-depth models, including age-depth temporal
17 uncertainties for 512 speleothems. SISALv2 is available at <http://dx.doi.org/10.17864/1947.242>[http://](http://doi.org/10.17864/1947.256)
18 doi.org/10.17864/1947.256 (Comas-Bru et al., ~~2020~~2020a).

19 **Copyright statement:** This dataset is licensed by the rights-holder(s) under a Creative Commons Attribution 4.0
20 International Licence: <https://creativecommons.org/licenses/by/4.0/>

21 **1. Introduction**

22 Speleothems (~~secondary cave carbonates form~~are a rich terrestrial palaeoclimate archive that forms from
23 infiltrating rainwater after it percolates through the soil, epikarst, and carbonate bedrock) ~~are a rich~~
24 ~~terrestrial palaeoclimate archive.~~ In particular, stable oxygen and carbon ~~isotope~~isotope ($\delta^{18}\text{O}$, $\delta^{13}\text{C}$)
25 measurements made on speleothems have been widely used to reconstruct regional and local
26 hydroclimate changes.

27 The Speleothem Isotope Synthesis and Analyses (SISAL) Working Group is an international effort, under
28 the auspices of Past Global Changes (PAGES), to compile speleothem isotopic records globally for the
29 analysis of past climates (Comas-Bru and Harrison, 2019). The first version of the SISAL database
30 (Atsawawaranunt et al., 2018a; Atsawawaranunt et al., 2018b) contained 381 speleothem records from
31 174 cave sites and has been used for analysing regional climate changes (Braun et al., 2019a; Burstyn et
32 al., 2019; Comas-Bru and Harrison, 2019; Deininger et al., 2019; Kaushal et al., 2018; Kern et al., 2019;
33 Lechleitner et al., 2018; Oster et al., 2019; Zhang et al., 2019). The potential for using the SISAL database
34 to evaluate climate models was explored using an updated version of the database (SISALv1b;
35 Atsawawaranunt et al., 2019) that contains 455 speleothem records from 211 sites (Comas-Bru et al.,
36 2019).

37 SISAL is continuing to expand the global database by including new records (Comas-Bru et al., ~~2020~~2020a).
38 Although most of the records in SISALv2 (79.7%: Figure 1a) have been dated using the generally very
39 precise, absolute radiometric $^{230}\text{Th}/\text{U}$ dating method, a variety of age-modelling approaches were
40 employed (Figure 1b) in constructing the original records. The vast majority of records provide no
41 information on the uncertainty of the age-depth relationship. However, many of the regional studies using
42 SISAL pointed to the limited statistical power of analyses of speleothem records because of the lack of
43 temporal uncertainties. For example, these missing uncertainties prevented the extraction of underlying
44 climate modes during the last 2k years in Europe (Lechleitner et al., 2018). To overcome this limitation,
45 we have developed additional age-depth models for the SISALv2 records (Figure 2) in order to provide
46 robust chronologies with temporal uncertainties. The results of the various age-depth modelling
47 approaches differ because of differences in their underlying assumptions. We have used seven alternative
48 methods: linear interpolation, linear regression, Bchron (Haslett and Parnell, 2008), Bacon (Blaauw, 2010;
49 Blaauw and Christen, 2011; Blaauw et al., 2019), OxCal (Bronk Ramsey, 2008, 2009; Bronk Ramsey and
50 Lee, 2013), COPRA (Breitenbach et al., 2012) and StalAge (Scholz and Hoffmann, 2011). Comparison of
51 these different approaches provides a robust measure of the age uncertainty associated with any specific
52 speleothem record.

53 **2. Data and Methods**

54 **2.1 Construction of age-depth models: the SISAL chronology**

55 We attempted to construct age-depth models for 533 entities in an automated mode. For eight records,
56 this automated construction failed for all methods. For these records we provide manually constructed
57 chronologies, where no age model previously existed, and added a note in the database with details on
58 the construction procedure. Age models for 21 records were successfully computed but later dropped in

59 the screening process due to inconsistent information or incompatibility for an automated routine. In
60 total, we provide ~~a new chronology~~additional chronologies for 512 speleothem records in SISALv2.

61 The SISAL chronology provides alternative age-depth models for SISAL records that are not composites
62 (i.e., time-series based on more than one speleothem record), that have not been superseded in the
63 database by a newer entity and which are purely $^{230}\text{Th}/\text{U}$ dated. We therefore excluded records for which
64 the chronology is based on lamina counting, radiocarbon ages or a combination of methods. This decision
65 was based on the low uncertainties of the age-depth models based on lamina counting and the challenge
66 of reproducing age-depth models based on radiocarbon ages. We made an exception with the case of
67 entity_id 163 (Talma et al., 1992), which covers two key periods, the Mid-Holocene and the Last Glacial
68 Maximum, at high temporal resolution. In this case, we calculated a new SISAL chronology based on the
69 provided $^{230}\text{Th}/\text{U}$ dates but did not consider the uncorrected ^{14}C ages upon which the original age-depth
70 model is based. We also excluded records for which isotopic data is not available (i.e., entities that are
71 part of composites) and entities that are constrained by less than three dates. Additionally, the dating
72 information for 23 entities shows hiatuses at the top/bottom of the speleothem that are not constrained
73 by any date. For these records, we partially masked the new chronologies to remove the unconstrained
74 section(s). Original dates were used without modification in the age-depth modelling.

75 To allow a comprehensive cross-examination of uncertainties, seven age-depth modelling techniques
76 were implemented here across all selected records. Due to the high number of records ($n = 533$), all
77 methods were run in batch mode. A preliminary study, using the database version v1b demonstrated the
78 feasibility of the automated construction and evaluation of age-depth models using a subset of records
79 and methods (Roesch and Rehfeld, 2019). Further details on the evaluation of the updated age-depth
80 models are provided in Section 3.2. The seven different methods are briefly described below. All methods
81 assume that growth occurred along a single growth axis. For one entity, where it was previously known
82 that two growth axes exist, we added an explanatory statement in the database. All approaches except
83 StalAge produce Monte Carlo (MC) iterations of the age-depth models. We ~~provide~~aimed at providing
84 1,000 MC iterations for each new SISALv2 chronology (<https://doi.org/10.5281/zenodo.3591197>), in
85 <http://doi.org/10.5281/zenodo.3816804> (Rehfeld et al., 2020) but this was not always possible because
86 some records (n=12) yield a substantial number of non-monotonic ensembles that were not kept.

87 Major challenges arise through hiatuses (growth interruptions) and age reversals. ~~h~~We developed a
88 workflow to deal with records with known hiatuses that allowed the classificationconstruction of age-
89 depth models for 20% of the records with one or more hiatuses (Roesch and Rehfeld, 2019; details below
90 for each age-depth modelling technique). Regarding the age reversals, we distinguish between tractable

91 reversals (with overlapping confidence intervals) and non-tractable reversals (i.e., where the two-sigma-
92 dating uncertainties do not overlap) following the definition of Breitenbach et al. (2012). ~~We developed a~~
93 ~~workflow to treat records with hiatuses (Roesch and Rehfeld, 2019; details below), which allowed the~~
94 ~~construction of age-depth models for 20% of the records with one or more hiatuses. Changes, Details~~ such
95 as the hiatus treatment and outlier age modification, are recorded in a logfile created when running the
96 age models. We followed the original author's choices ~~with regard to~~ regarding date usage. If an age was
97 marked as "not used" or "usage unknown", we did not consider this in the construction of the new
98 chronologies except in OxCal, where dates with "usage unknown" were considered.

99 1) **Linear Interpolation** (*lin_interp_age*) between radiometric dates. This is the classic approach for age-
100 depth model construction for palaeoclimate archives and was used in 32.1% of the original age-depth
101 models in SISALv2. Here, we extend this approach and calculate the age uncertainty by sampling the range
102 of uncertainty of each $^{230}\text{Th}/\text{U}$ -age 2,000 times, assuming a Gaussian distribution. This approach is
103 consistent with the implementation of linear interpolation in CLAM (Blaauw, 2010) and COPRA
104 (Breitenbach et al., 2012). Linear interpolation was implemented in R (R Core Team, 2019), using the
105 `approxExtrap()` function in the `Hmisc` package. We included an automated reversal check that
106 increases the dating uncertainties until a monotonic age model is achieved, similar to that of `StalAge`
107 (Scholz and Hoffmann, 2011). Hiatuses are modelled following the approach of Roesch and Rehfeld (2019),
108 where rather than modelling each segment separately, synthetic ages with uncertainties spanning the
109 entire hiatus duration are introduced for use in age-depth model construction. These synthetic ages are
110 removed after age-depth model construction. Linear interpolation was applied to 80% (n=408/512) of the
111 SISAL records for which new chronologies were developed.

112 2) **Linear Regression** (*lin_reg_age*) provides a single best fit line through all available radiometric ages
113 assuming a constant growth rate. Linear regression was used in 6.7% of the original SISALv2 age models.
114 As with linear interpolation, age uncertainties are based on randomly sampling the U-series dates to
115 produce 2,000 age-depth models (i.e., ensembles). Temporal uncertainties are then given by the
116 uncertainty of the median-based fit to each ensemble member. If hiatuses are present, the segments in-
117 between were split at the depth of the hiatus without an artificial age. The method is implemented in R,
118 using the `lm()` function from the base package. Linear regression was applied to 36% (n=185/512) of the
119 SISAL records for which new chronologies were developed.

120 3) **Bchron** (*Bchron_age*) is a Bayesian method based on a continuous Markov processes (Haslett and
121 Parnell, 2008) and available as an R package (Parnell, 2018). This method was originally used for only one
122 speleothem record in SISALv2. Since *Bchron* cannot handle hiatuses, we implemented a new workflow

123 that adds synthetic ages with uncertainties spanning the entire hiatus duration (Roesch and Rehfeld,
124 2019), as performed with linear interpolation, StalAge and our implementation of COPRA. Bchron provides
125 age-depth model ensembles of which we have kept the last 2,000. We calculate the age uncertainties
126 from the spread of the individual ensembles. Here we use the function `bchron()` with
127 `jitter.positions = true` to mitigate problems due to rounded-off depth values. This method
128 has been applied to 83% (n=426/512) of the SISAL records for which new chronologies were developed.

129 4) **Bacon** (*Bacon_age*) is a semi-parametric Bayesian method based on autoregressive gamma-processes
130 (Blaauw, 2010; Blaauw and Christen, 2011; Blaauw et al., 2019). It was used in three of the original
131 chronologies in SISALv2. The R package *rBacon* can handle both outliers and hiatuses and apart from
132 giving the median age-depth model, it also returns the Monte Carlo realisations (i.e. ensembles), from
133 which the median age-depth model is calculated. During the creation of the SISAL chronologies, the
134 existing *rBacon* package (version 2.3.9.1) was updated to improve the handling of stalagmite growth rates
135 and hiatuses. We use this revised version, available on CRAN ([https://cran.r-](https://cran.r-project.org/web/packages/rbacon/index.html)
136 [project.org/web/packages/rbacon/index.html](https://cran.r-project.org/web/packages/rbacon/index.html)), [https://cran.r-](https://cran.r-project.org/web/packages/rbacon/index.html)
137 [project.org/web/packages/rbacon/index.html](https://cran.r-project.org/web/packages/rbacon/index.html); last access date: 31 January 2020), to provide a median
138 age-depth model and an ensemble of age-model realisations for 65% (n=335/512) of the SISAL records for
139 which new chronologies were developed.

140 5) **OxCal** (*Oxcal_age*) is a Bayesian chronological modelling tool that uses Markov Chain Monte Carlo
141 (Bronk Ramsey, 2009). This method was used in 4.1% of the original SISALv2 chronologies. OxCal can deal
142 with hiatuses and outliers and accounts for the non-uniform nature of the deposition process (Poisson
143 process using the P_Sequence command). Here we used the analysis module of OxCal version 4.3 with a
144 default initial value of interpolation rate of 1 and an initial value of model rigidity (k) of $k_0=1$ with a uniform
145 distribution from 0.01 to 100 for the range of k/k_0 ($\log_{10}(k/k_0)=(-2,2)$) (~~C.~~ Christoph Bronk Ramsey,
146 personal communication, 2019). The initial value of the interpolation rate determines the number of
147 points between any two dates, for which an age will be calculated. We subsequently linearly interpolated
148 the age-depth model to the depths of individual isotope measurements. WereWhere multiple dates are
149 given for the same depth for any given entity, the date with the smallest uncertainty was used to construct
150 the SISAL chronology. In case of asymmetric uncertainties in the dating table, the largest uncertainty value
151 was chosen. We kept the last 2,000 realisations of the age-depth models for each entity. We calculate the
152 age uncertainties from the spread of the individual ensembles. Details of the workflow used to construct
153 these chronologies are available at Amirnezhad-Mozhdehi and Comas-Bru (2019). OxCal chronologies are
154 available for 21% (n=106/512) of the SISAL records for which new chronologies were developed.

155 6) **COPRA** (*copRa_age*) is an approach based on interpolation-between-dates (Breitenbach et al., 2012)
156 and was used for 9.7% of the original SISALv2 chronologies. COPRA is available as a Matlab package [in](#)
157 [Rehfeld et al. \(2017\)](#) with a graphical user interface (GUI) that has interactive checks for reversals and
158 hiatuses. The Matlab version can handle multiple hiatuses and (to some extent) layer-counted segments.
159 However, age-reversals can occur near short-lived hiatuses. To overcome this, we implemented a new
160 workflow in R that adds artificial dates at the location of the hiatuses and prevents the creation of age
161 reversals (Roesch and Rehfeld, 2019) as done with linear interpolation, StalAge and Bchron. Additionally,
162 we also incorporated an automated reversal check similar to that already embedded into StalAge (Scholz
163 and Hoffmann, 2011). This R version, *copRa*, uses the default piecewise-cubic-hermite-interpolation
164 (*pchip*) algorithm in R without consideration of layer counting. [We calculate the age uncertainties from](#)
165 [the spread of the individual ensembles](#). This approach was used for 76% (n= 389/512) of the SISAL records
166 for which new chronologies were developed.

167 7) **StalAge** (*StalAge_age*) fits straight lines through three adjacent dates using weights based on the dating
168 measurement errors (Scholz and Hoffmann, 2011). Age uncertainties are iteratively obtained through a
169 Monte Carlo approach, but ensembles are not given in the output. StalAge was used to construct 13.1%
170 of the original SISALv2 chronologies. The StalAge v1.0 R function has been updated to R version 3.4 and
171 the default outlier and reversal checks were enabled to run automatically. Hiatuses cannot be entered in
172 StalAge v1.0, but the updated version incorporates a treatment of hiatuses based on the creation of
173 temporary synthetic ages following Roesch and Rehfeld (2019). In contrast to other methods, mean ages
174 instead of median ages are reported for StalAge-[and the uncertainties are internally calculated and based](#)
175 [on iterative fits considering dating uncertainties](#). StalAge was applied to 62% (n=320/512) of the SISAL
176 records for which new chronologies were developed.

177 **2.2 Revised structure of the database**

178 The data are stored in a relational database (MySQL), which consists of 15 linked tables: *site*, *entity*,
179 *sample*, *dating*, *dating_lamina*, *gap*, *hiatus*, *original_chronology*, *d13C*, *d18O*, *entity_link_reference*,
180 *references*, *composite_link_entity*, *notes* and *sisal_chronology*. Figure 3 shows the relationships between
181 these tables and the type of each field (e.g. numeric, text). The structure and contents of all tables except
182 the new *sisal_chronology* table are described in detail in Atsawawaranunt et al. (2018a). Here, we focus
183 on the new *sisal_chronology* table and on the changes that were made to other tables in order to
184 accommodate this new table (See section 2.3). Details of the fields in this new table are listed in Table 1.

185 Changes were also made to the dating table (*dating*) to accommodate information about whether a
186 specific date was used to construct each of the age-depth models in the *sisal_chronology* table (Table 2).

187 We followed the original authors' decision regarding the exclusion of dates (i.e. because of high
188 uncertainties, age reversals or high detrital content). However, some dates used in the original age-depth
189 model were not used in the SISALv2 chronologies to prevent unrealistic age-depth relationships (i.e. age
190 inversions). Information on whether a particular date was used for the construction of specific type of
191 age-depth model is provided in the dating table, under columns labelled *date_used_lin_interp*,
192 *date_used_lin_reg*, *date_used_Bchron*, *date_used_Bacon*, *date_used_OxCal*, *date_used_copRa* and
193 *date_used_StalAge* (Table 2).

194 The dating and the sample tables were modified to accommodate the inclusion of new entities in the
195 database. Specifically, the pre-defined options lists were expanded, options that had never been used
196 were removed, and some typographical errors in the field names were corrected; these changes are listed
197 in Table 3.

198 **3. Quality Control**

199 **3.1 Quality control of individual speleothem records**

200 The quality control procedure for individual records newly incorporated in the SISALv2 database is based
201 on the steps described in Atsawawaranunt et al. (2018a). We have updated the Python database scripts
202 to provide a more thorough quality assessment of individual records. Additional checks of the dating table
203 resulted in modifications in the *230Th_232Th*, *230Th_238U*, *234U_238U*, *ini230Th_232Th*, *238U_content*,
204 *230Th_content*, *232Th_content* and *decay constant* fields in the dating table for 60 entities. A summary
205 of the fields that are both automatically and manually checked before uploading a record to the database
206 is available in Appendix 1.

207 Analyses of the data included in SISALv1 (Braun et al., 2019a; Burstyn et al., 2019; Deininger et al., 2019;
208 Kaushal et al., 2018; Kern et al., 2019; Lechleitner et al., 2018; Oster et al., 2019; Zhang et al., 2019) and
209 SISALv1b (Comas-Bru et al., 2019) revealed a number of errors in specific records that have now been
210 corrected. These revisions include, for example, updates in mineralogies (*sample.mineralogy*), revised
211 coordinates (*site.latitude* and/or *site.longitude*) and addition of missing information that was previously
212 entered as "unknown". The fields affected and the number of records with modifications are listed in
213 Table 4. All revisions are also documented at Comas-Bru et al., ~~2020.~~ (2020a).

214 **3.2 ~~Quality~~Automation and quality control of the age-depth models in the SISAL chronology**

215 ~~The conception and the test of the R workflow, integrating all methods but OxCal, was outlined in Roesch~~
216 ~~and Rehfeld (2019) and includes automatized checks for the final chronologies except for OxCal. We used~~
217 ~~an automated approach to age-depth modelling in R because of the large number of records. Roesch and~~

218 Rehfeld (2019) have described the basic workflow concept and tested it using all of the age-modelling
219 approaches used here except OxCal. The basic workflow involves step-by-step inspection and formatting
220 of the data for the different methods, and the use of pre-defined parameter choices specific to each
221 method. Each age-modelling method is called sequentially. An error message is recorded in the log file if
222 a particular age-modelling method fails, and the algorithm then progresses to the next method. If output
223 is produced for a particular age-modelling method, these age models are checked for monotonicity.
224 Finally, the output standardization routine writes out, for each entity and age-modelling approach, the
225 median age model, the ensembles (if applicable) and information of which hiatuses and dates were used
226 in the construction of the age models. These outputs are then added to the sisal chronology table (Table
227 2). All functions are available at <https://github.com/paleovar/SISAL.AM> (last access: 23 July 2020) and
228 CRAN (<https://cran.r-project.org/web/packages/rbacon/index.html>; last access: 31 January 2020).

229 The general approach for the OxCal age models was similar, and step-by-step details and scripts are
230 provided in <https://doi.org/10.5281/zenodo.3586280> (Amirnezhad-Mozhdehi and Comas-Bru, 2019). The
231 quality control parameters obtained from OxCal were compared with the recommended values of
232 Agreement Index (A) > 60% and Convergence (C) > 95%, in accordance with the guidelines in Bronk Ramsey
233 (2008). ~~In addition to,~~ both for the overall model agreement and P_Sequence convergence meeting these
234 criteria, for at least 90% of the individual dates ~~had to have an acceptable Agreement and Convergence~~
235 ~~themselves.~~ OxCal age-depth models failing to meet these criteria were not included in the SISAL
236 sisal chronology table. ~~(Table 2).~~

237 An overview of the evaluation results for the age-depth models constructed in automated mode is given
238 in Figure 4. Three nested criteria are used to evaluate them. Firstly, chronologies with reversals (Check 1)
239 are automatically rejected (score -1). Secondly, the final chronology should flexibly follow clear growth
240 rate changes (Check 2), such that 70% of the dates are encompassed in the final age-depth model within
241 4 sigma uncertainty (score +1). Thirdly, temporal uncertainties are expected to increase between dates
242 and near hiatuses (Check 3). This criterion is met in the automated screening (score +1) if the Interquartile
243 range (IQR) is higher between dates or at hiatuses than at dates. Only entities that pass all three criteria
244 are considered successful. All age-depth models that satisfied Check 1 were also evaluated in an expert-
245 based manual screening by ten people. If more than two experts agreed that an individual age-depth
246 model was unreliable or inconsistencies, such as large offsets between the original age model and the
247 dates marked as 'used', occurred, the model was not included in the SISAL chronology table. This
248 automatic and expert-based quality control screening resulted in 2,138 new age-depth models
249 constructed for 503 SISAL entities.

250 4. Recommendation for the use of SISAL chronologies

251 The original age-depth models for every entity are available in SISALv2. However, given the lack of age
252 uncertainties for most of the records, we recommend considering the SISAL chronologies with their
253 respective 95% confidence intervals whenever possible. No single age-depth modelling approach is
254 successful for all entities, and we therefore recommend that all the methods for a specific entity are used
255 together in visual and/or statistical comparisons. Depending on methodological choices, age-depth
256 models compatible with the dating evidence can result in considerable temporal differences for
257 transitions (Figure 5). For analyses relying on the temporal alignment of records (e.g. cross-correlation),
258 age-depth model uncertainties should be considered using the ensemble of compatible age-depth models
259 as described, e.g., in Mudelsee et al. (2012), Rehfeld and Kurths (2014) and Hu et al. (2017).

260 5. Overview of database contents

261 SISALv2 contains 353,976 $\delta^{18}\text{O}$ and 200,613 $\delta^{13}\text{C}$ measurements from 673 individual speleothem records
262 and 18 composite records from 293 cave [systemsites](#) (Table 5; Figure 2; Comas-Bru et al., [2020a](#)).
263 There are 20 records included in SISALv2 that are identified as being superseded and linked to the newer
264 records; their original datasets are included in the database for completeness. This is an improvement of
265 235 records from SISALv1b (Atsawawaranunt et al., 2019; Comas-Bru et al., 2019; Table 6). SISALv2
266 represents 72% of the existing speleothem records identified by the SISAL Working Group and more than
267 three times the number of speleothem records in the NCEI-NOAA repository (n = 210 as of November
268 2019), which is the one most commonly used by the speleothem community to make their data publicly
269 available. SISALv2 also contains nine records that have not been published or are only available in PhD
270 theses.

271 The published age-depth models of all speleothems are accessible in the *original_chronology* metadata
272 table and our standardised age-depth models are available at the *sisal_chronology* table for 512
273 speleothems. Temporal uncertainties are now provided for 79% of the records in the SISAL database. [This
274 is a significantly larger number than in SISALv1b, where most age-depth models lacked temporal
275 uncertainties. Most speleothem records show average U-Th age errors between 100-1,000 years \(Figure
276 6\), which are only slightly changed by using age-depth modelling software. Nevertheless, when comparing
277 the mean uncertainties of the U-Th ages with those of their corresponding age-depth model, the slope
278 between both parameters is smaller than one. This indicates that age-depth models tend to reduce
279 uncertainties especially when dating errors are large while they increase uncertainties, when U-Th age
280 errors are small.](#)

281 This second version of the SISAL database has an improved spatial coverage compared to SISALv1
282 (Atsawawaranunt et al., 2018b) and SISALv1b (Figure 3; Atsawawaranunt et al., 2019). SISALv2 contains
283 most published records from Oceania (80.2%), Africa (73.7%) and South America (77.6%), but
284 improvements are still possible in regions like the Middle East (42.3%) and Asia (64.8%) (Table 6).

285 The temporal distribution of records for the past 2,000 years is good, with 181 speleothems covering at
286 least one-third of this period and 84 records covering the entire last 2k (-68 to 2,000 years BP) with an
287 average resolution of 20 isotope measurements in every 100-year slice (Figure 6a7a). There are 182
288 records that cover at least one-third of the Holocene (last 11,700 years BP) with 37 of these covering the
289 whole period with at least one isotope measurement in every 500-year period (Figure 6b7b). There are
290 84 entities during the deglaciation period (21,000 to 11,700 years BP) with at least one measurement in
291 every 500-year time period (Figure 6b7b). The Last Interglacial (130,000 to 115,000 years BP) is covered
292 by 47 speleothem records that record at least one-third of this period with, on average, 25 isotope
293 measurements at every 1,000-year time-slice (Fig. 6cFigure 7c).

294 This updated SISALv2 database now provides the basis not only for comparing a large number of
295 speleothem-based environmental reconstructions on regional to a global scale, but also allows for
296 comprehensive analyses of stable isotope records on various timescales from multi-decadal to orbital.

297 **6. Data and code availability:**

298 The database is available in SQL and CSV format from
299 <http://dx.doi.org/10.17864/1947.242><https://dx.doi.org/10.17864/1947.256> (Comas-Bru et al.,
300 20202020a). The code used for constructing the linear interpolation, linear regression, Bchron, Bacon,
301 copRa and StalAge age-depth models is available at
302 <https://github.com/palaeovar/SISAL.AM><https://github.com/paleovar/SISAL.AM> (last access: 23 July
303 2020). rBacon package (version 2.3.9.1) is available on CRAN ([https://cran.r-](https://cran.r-project.org/web/packages/rbacon/index.html)
304 [project.org/web/packages/rbacon/index.html](https://cran.r-project.org/web/packages/rbacon/index.html))[https://cran.r-](https://cran.r-project.org/web/packages/rbacon/index.html)
305 [project.org/web/packages/rbacon/index.html](https://cran.r-project.org/web/packages/rbacon/index.html); last access: 31 January 2020). The code used to construct
306 the OxCal age-depth models and trim the ensembles output to the last 2,000 iterations is available at
307 <https://doi.org/10.5281/zenodo.3586280><https://doi.org/10.5281/zenodo.3586280> (Amirnezhad-
308 Mozhdghi and Comas-Bru, 2019). The ensembles are available at
309 <https://doi.org/10.5281/zenodo.3591197><https://doi.org/10.5281/zenodo.3816804> (Rehfeld et al.,
310 2020). The workbook used to submit data to SISAL ~~is available and the codes for its quality assessment~~
311 ~~are available at~~ <https://doi.org/10.5281/zenodo.3631403> (Atsawawaranunt and Comas-Bru, 2020). The
312 ~~workbook is also available~~ as a supplementary document of Comas-Bru and Harrison (2019); ~~also available~~

313 at <https://10.5281/zenodo.3631403>. The codes for the quality control assessment of the data submitted
314 to SISAL can be obtained from <https://10.5281/zenodo.3631403>. The codes to assess the dating table in
315 SISALv2 are available at https://github.com/jensfohlmeister/QC_SISALv2_dating_metadata (last access:
316 23 July 2020) and https://github.com/jensfohlmeister/QC_SISALv2_dating_metadata and
317 <https://10.5281/zenodo.3631443>.<https://10.5281/zenodo.3631443> (Comas-Bru et al., 2020b). Details on
318 the Quality Control assessments are available in the Supplementary material.

319 **Author contributions:**

320 LCB is the coordinator of the SISAL working group. LCB, SPH and KR designed the new version of the
321 database. KR coordinated the construction of the new age-depth models except OxCal. All age-depth
322 models except OxCal were run by CR and KR. LCB coordinated the construction of the OxCal age-depth
323 models, which were run by SAM and LCB. LCB implemented the changes in the v2 of the database with
324 the assistance of KA, SMA, YAB, AB, YB, MB, AC, MD, AD, BD, IGH, JH, NK, ZK, FAL, AL, BM, VFN, JO, CPM,
325 NS, NS, BMW, SW and HZ coordinated the regional data collection and the age-model screening. SFMB,
326 MB and DS provided support for COPRA, Bacon and StalAge, respectively. JF assisted in the Quality Control
327 procedure of the SISAL database. Figures 1, 4 and 5 were created by CR and KR. Figures 2, 3 and 6 were
328 created by LCB. All authors listed as “SISAL Working Group members” provided data for this version of the
329 database and/or helped to complete data entry. The first draft of the paper was written by LCB with inputs
330 by KR and SPH and all authors contributed to the final version.

331 **Team list:**

332 The following SISAL Working Group members contributed with ~~data~~[either data or age-modelling advice](#)
333 to SISALv2: James Apaéstegui (Instituto Geofísico del Perú, Lima, Peru), Lisa M. Baldini (School of Health
334 & Life Sciences, Teesside University, Middlesbrough, UK), Shraddha Band (Geoscience Department,
335 National Taiwan University, No.1, Sec. 4, Roosevelt Road, Taipei 106, Taiwan), Maarten Blaauw (School of
336 Natural and Built Environment, Queen's University Belfast, U.K.), Ronny Boch (Institute of Applied
337 Geosciences, Graz University of Technology, Rechbauerstraße 12, 8010 Graz, Austria), Andrea Borsato
338 (School of Environmental and Life Sciences, University of Newcastle, Callaghan 2308, NSW, Australia),
339 Alexander Budsky (Institute for Geosciences, Johannes Gutenberg University Mainz, Johann-Joachim-
340 Becher-Weg 21, 55128 Mainz, Germany), Maria Gracia Bustamante Rosell (Department of Geology and
341 Environmental Science, University of Pittsburgh, USA), Sakonvan Chawchai (Department of Geology,
342 Faculty of Science, Chulalongkorn University, Bangkok 10330, Thailand), Silviu Constantin (Emil Racovita
343 Institute of Speleology, Bucharest, Romania and Centro Nacional de Investigación sobre la Evolución

344 Humana, CENIEH, Burgos, Spain), Rhawn Denniston (Department of Geology, Cornell College, Mount
345 Vernon, IA 52314, USA), Virgil Dragusin (Emil Racovita Institute of Speleology, 010986, Strada Frumoasă
346 31, Bucharest, Romania), Russell Drysdale (School of Geography, University of Melbourne, Melbourne,
347 Australia), Oana Dumitru (Karst Research Group, School of Geosciences, University of South Florida, 4202
348 E. Fowler Ave., NES 107, Tampa, FL 33620, USA), Amy Frappier (Department of Geosciences, Skidmore
349 College, Saratoga Springs, New York, USA), Naveen Gandhi (Indian Institute of Tropical Meteorology, Dr.
350 Homi Bhabha Road, Pashan, Pune-411008, India), Pawan Gautam (Centre for Earth, Ocean and
351 Atmospheric Sciences, University of Hyderabad, India; now at Geological Survey of India, Northern Region,
352 India), Li Hanying (Institute of Global Environmental Change, Xi'an Jiaotong University, China), Ilaria Isola
353 (Istituto Nazionale di Geofisica e Vulcanologia, Pisa, Italy), Xiuyang Jiang (College of Geography Science,
354 Fujian Normal University, Fuzhou 350007, China), Zhao Jingyao (Institute of Global Environmental Change,
355 Xi'an Jiaotong University, China), Kathleen Johnson (Dept. of Earth System Science, University of
356 California, Irvine, 3200 Croul Hall, Irvine, CA 92697 USA), Vanessa Johnston (Research Centre of Slovenian
357 Academy of Sciences and Arts ZRC SAZU, Novi trg 2, Ljubljana, Slovenia), Gayatri Kathayat (Institute of
358 Global Environmental Change, Xi'an Jiaotong University, China), Jennifer Klose (Institut für
359 Geowissenschaften, Johannes Gutenberg-Universität Mainz, Germany), Claire Krause (Geoscience
360 Australia, Canberra, Australian Capital Territory, 2601, Australia), Matthew Lachniet (Department of
361 Geoscience, University of Nevada Las Vegas, Las Vegas, NV 89154), Amzad Laskar (Geosciences Division,
362 Physical Research Laboratory, Navrangpura, Ahmedabad 380009, India), Stein-Erik Lauritzen (University
363 of Bergen, Earth science, Norway), Nina Loncar (University of Zadar, Department of Geography, 23000,
364 Ulica Mihovila Pavlinovića, Zadar, Croatia), Gina Moseley (Institute of Geology, University of Innsbruck,
365 Innrain 52, 6020 Innsbruck, Austria), Allu C Narayana (Centre for Earth, Ocean and Atmospheric Sciences,
366 University of Hyderabad, India), Bogdan P. Onac (University of South Florida, School of Geosciences, 4202
367 E Fowler Ave, Tampa, FL 33620, USA, Emil Racovita Institute of Speleology, Cluj-Napoca, Romania), Jacek
368 Pawlak (Institute of Geological Sciences, Polish Academy of Sciences, 00-818, Twarda 51/55, Warsaw,
369 Poland), Christopher Bronk Ramsey (Research Laboratory for Archaeology and the History of Art, Oxford
370 University, Oxford, UK), Isabel Rivera-Collazo (Department of Anthropology and the Scripps Institution of
371 Oceanography, UC San Diego, USA), Carlos Rossi (Dept. Petrología y Geoquímica, Facultad de Ciencias
372 Geológicas, Universidad Complutense, Madrid, Spain), Peter J. Rowe (School of Environmental Sciences,
373 University of East Anglia, NR4 7TJ, Norwich Research Park, Norwich, UK), Nicolás M. Stríkis (Department
374 of Geochemistry, Universidade Federal Fluminense, Niterói, Brazil), Liangcheng Tan (State Key Laboratory
375 of Loess and Quaternary Geology, Institute of Earth Environment, Chinese Academy of Sciences, Xi'an
376 710075, China), Sophie Verheyden (Politique scientifique fédérale belge BELSPO, Bvd. Simon Bolivar
377 30,1000 Brussels), Hubert Vonhof (Max Planck Institute for Chemistry, Mainz, Germany), Michael Weber

378 (Johannes Gutenberg-Universität Mainz, Germany), Kathleen Wendt (~~Geo- und~~
379 ~~Atmosphärenwissenschaften, Universität~~Institute of Geology, University of Innsbruck, Austria), Paul
380 Wilcox (Institute of Geology, University of Innsbruck, Austria), Amos Winter (Dept. of Earth and
381 Environmental Systems, Indiana State University, USA), Jiangying Wu (School of Geography, Nanjing
382 Normal University, Nanjing, China), Peter Wynn (Lancaster Environment Centre, University of Lancaster,
383 Lancaster, LA1 4YQ UK), Madhusudan G. Yadava (Geosciences Division, Physical Research Laboratory,
384 Navrangpura, Ahmedabad 380009, India).

385 **Competing Interests:**

386 The authors declare no competing interests.

387 **Funding:**

388 SISAL (Speleothem Isotopes Synthesis and Analysis) is a working group of the Past Global Changes (PAGES)
389 programme. We thank PAGES for their support for this activity. The design and creation of v2 of the
390 database was supported by funding to SPH from the ERC-funded project GC2.0 (Global Change 2.0:
391 Unlocking the past for a clearer future, grant number 694481) and the Geological Survey Ireland Short Call
392 2017 (Developing a toolkit for model evaluation using speleothem isotope data, grant number 2017-SC-
393 056) award to LCB. SPH and LCB acknowledge additional support from the ERC-funded project GC2.0 and
394 from the JPI-Belmont project “PALaeo-Constraints on Monsoon Evolution and Dynamics (PACMEDY)”
395 through the UK Natural Environmental Research Council (NERC). KR and DS acknowledge support by the
396 Deutsche Forschungsgemeinschaft (DFG, codes RE3994/2-1 and SCHO 1274/11-1).

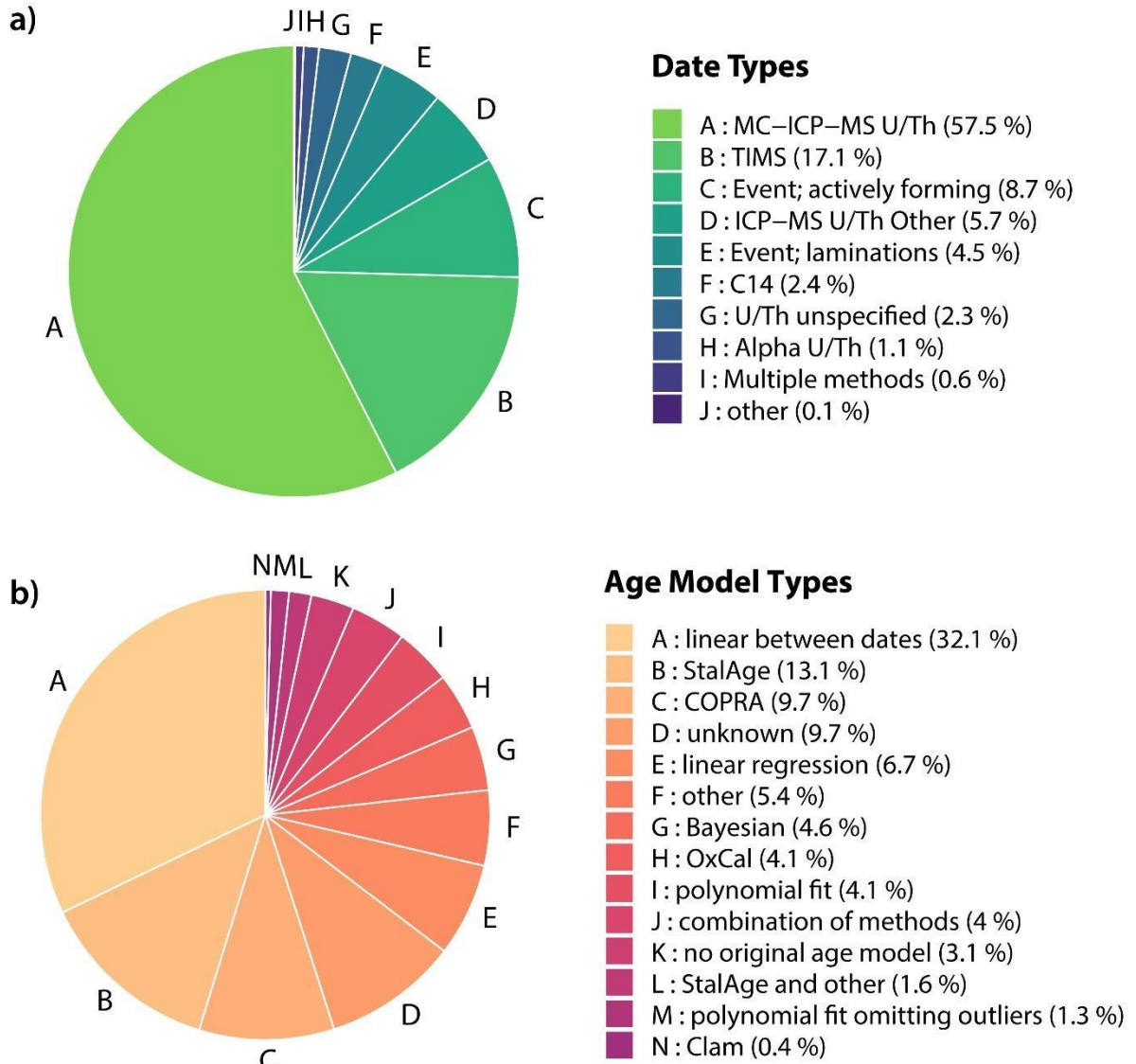
397 **Acknowledgements**

398 SISAL (Speleothem Isotopes Synthesis and Analysis) is a working group of the Past Global Changes (PAGES)
399 programme. We thank PAGES for their support for this activity. We thank SISAL members who
400 contributed their published data to the database and provided additional information when necessary.
401 We thank all experts who engaged in the age-depth model evaluation. The authors would like to
402 acknowledge Avner Ayalon, Jordi López, Bahadur Singh Kotlia, ~~and~~ Dennis Rupprecht.

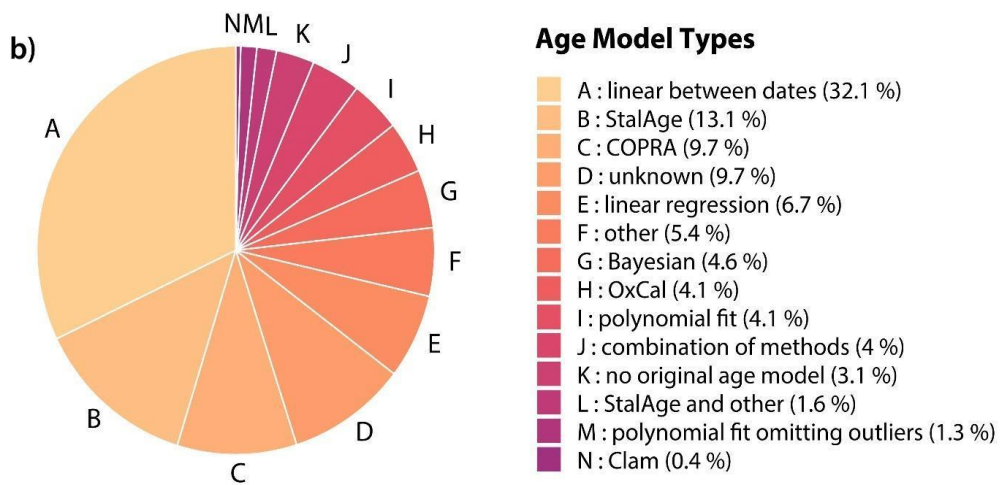
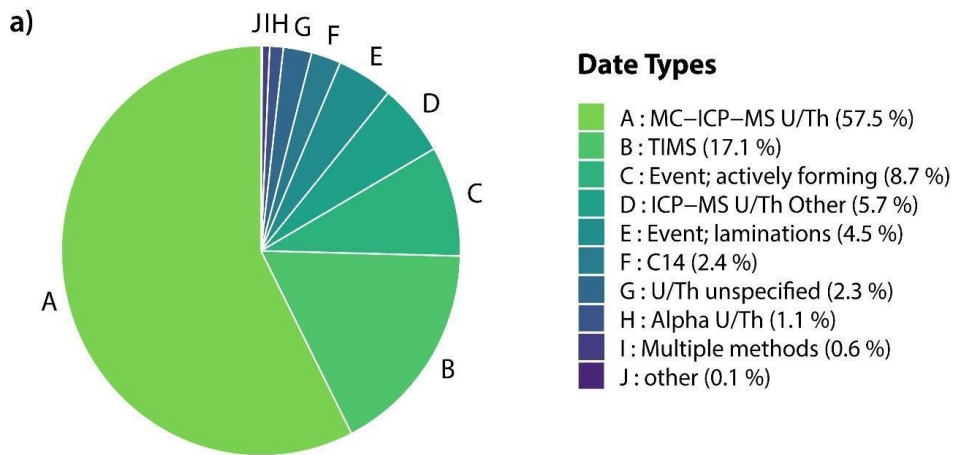
403

404 **List of Figures and Tables**

405 **Figure 1:** Summary of the dating information on which the original age-depth models are based
 406 (a) and the original age-depth model types (b) present in SISALv2.
 407

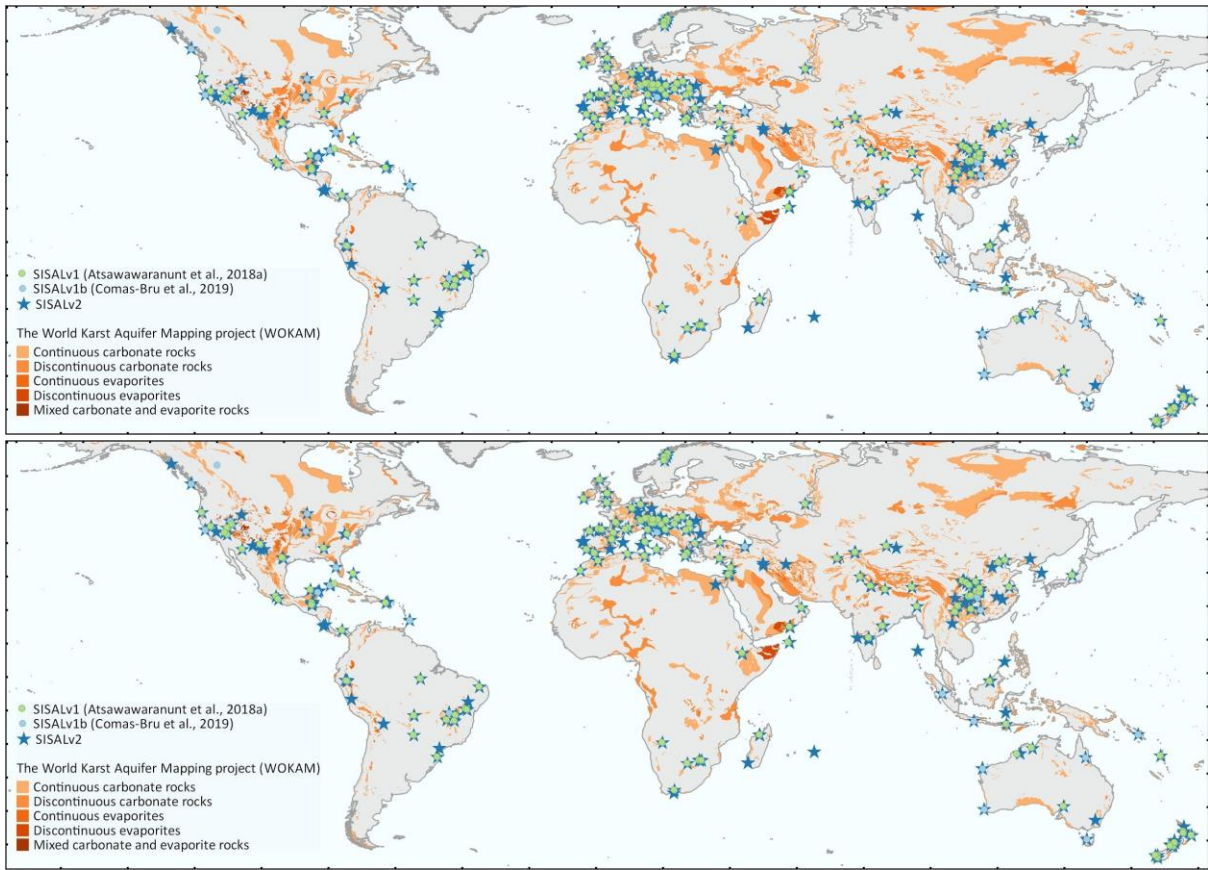


408
409



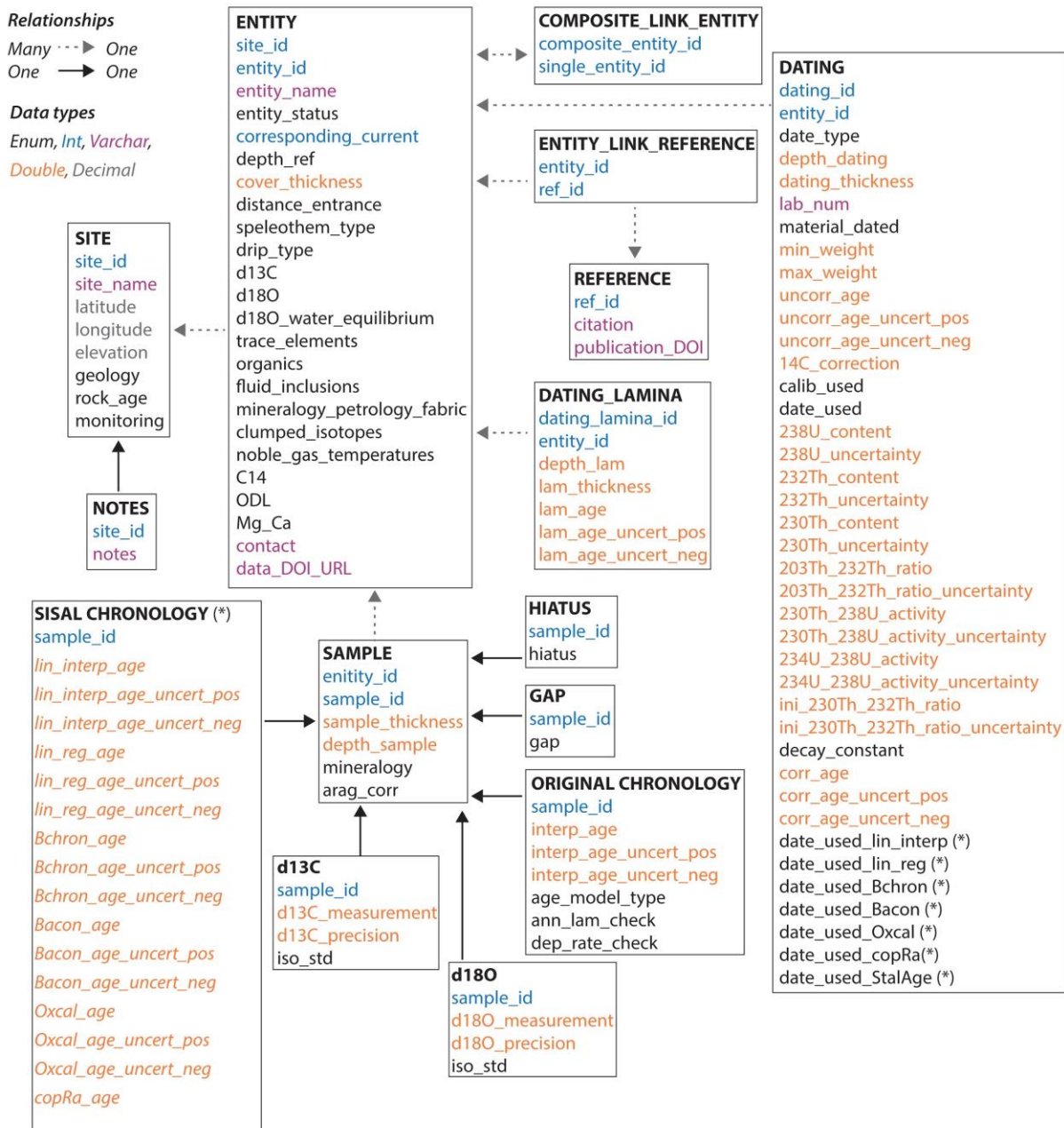
410
411
412

413 **Figure 2:** Cave sites included in the version 1, 1b and 2 of the SISAL database on the Global Karst
414 Aquifer Map (WOKAM ~~project; Chen et al., 2017: [https://www.un-igrac.org/resource/world-](https://www.un-igrac.org/resource/world-
415 karst-aquifer-map-wokam)~~
~~[karst-aquifer-map-wokam](https://www.un-igrac.org/resource/world-karst-aquifer-map-wokam); Goldscheider et al., 2020~~).

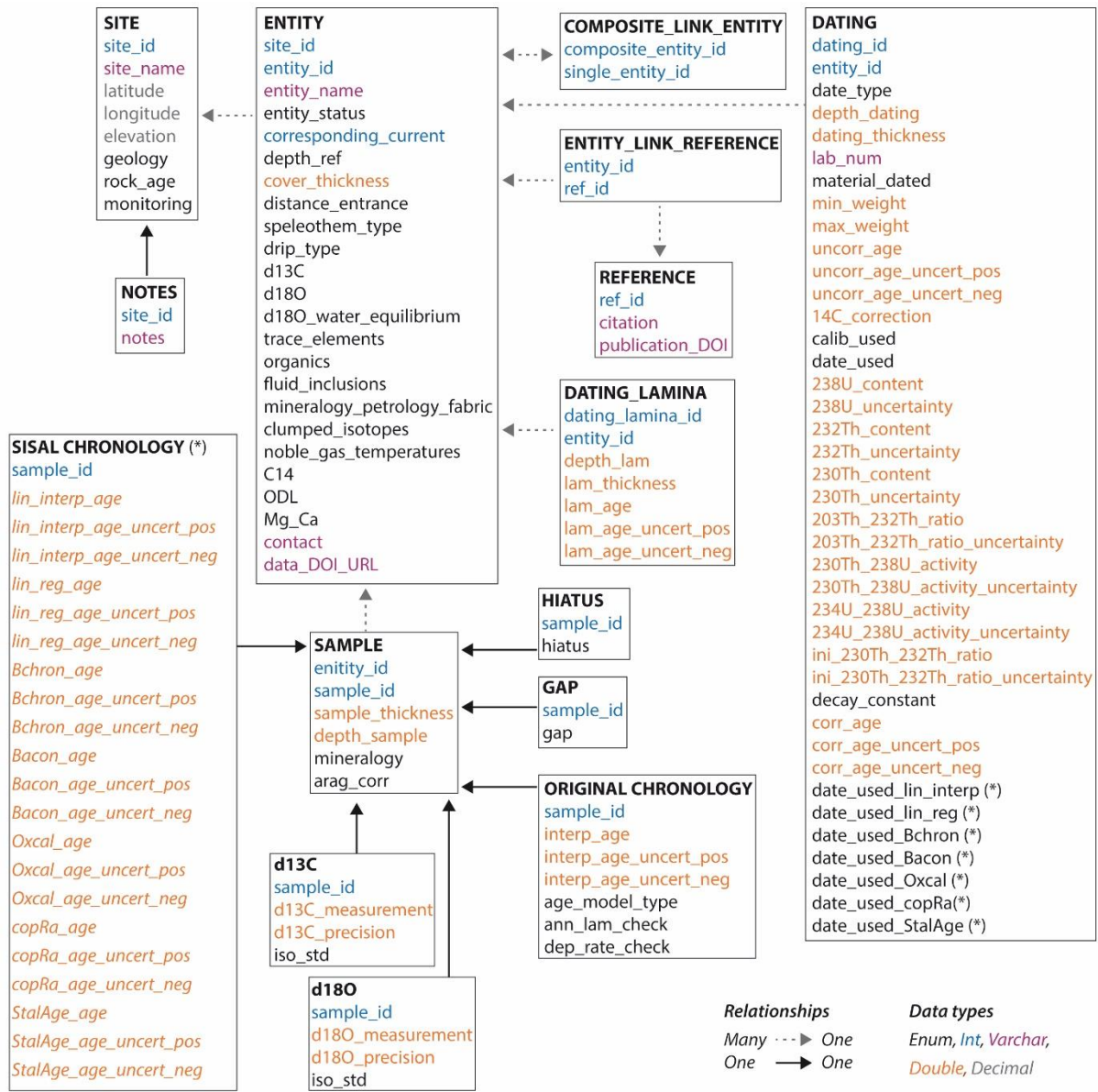


419 **Figure 3:** The structure of the SISAL database version 2. Fields and table marked with (*) refer to
 420 new information added to SISALv1b; see tables 1 and 2 for details. The colours refer to the format
 421 of that field: Enum, Int, Varchar, Double or Decimal. More information on the list of pre-defined
 422 menus can be found in Atsawawaranunt et al. (2018a).

423

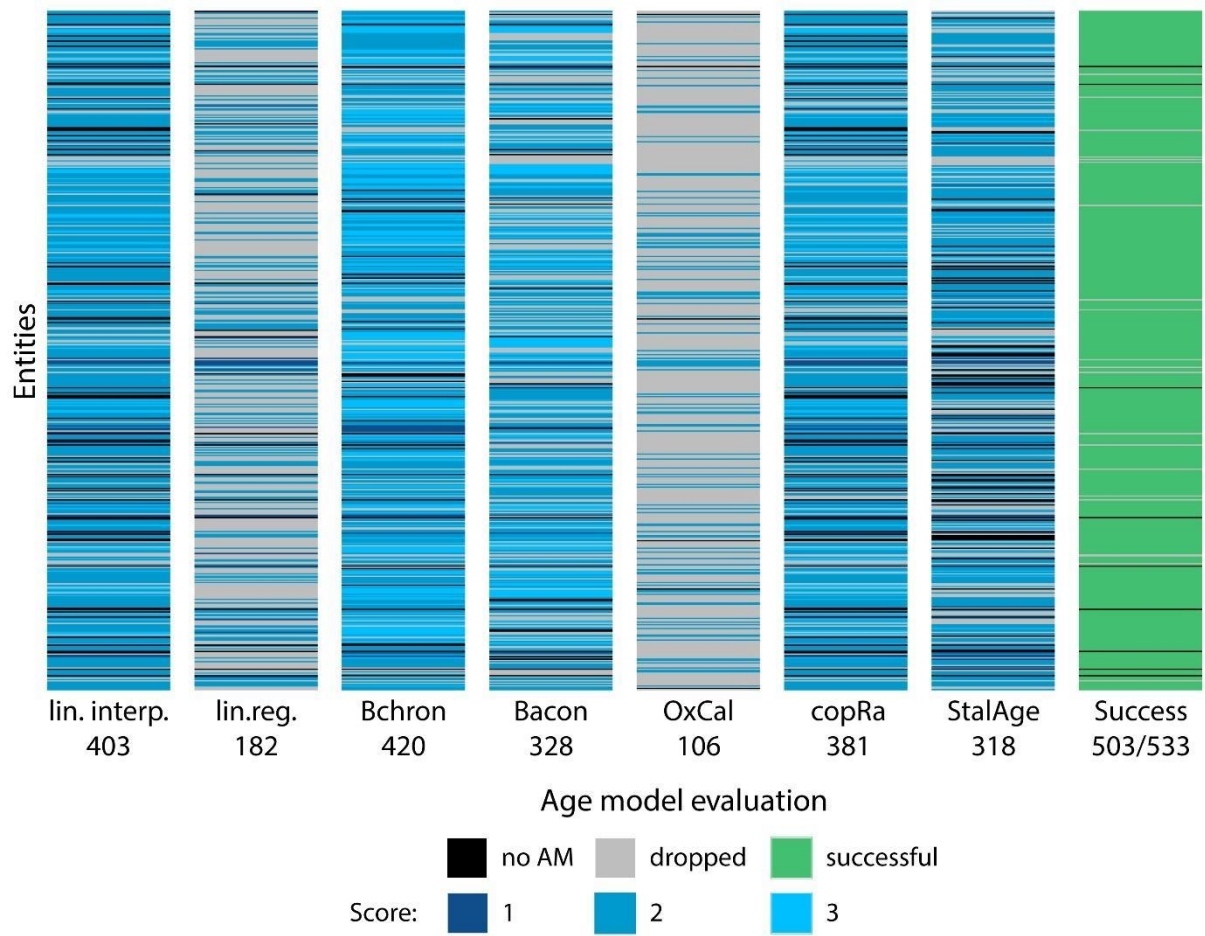


424

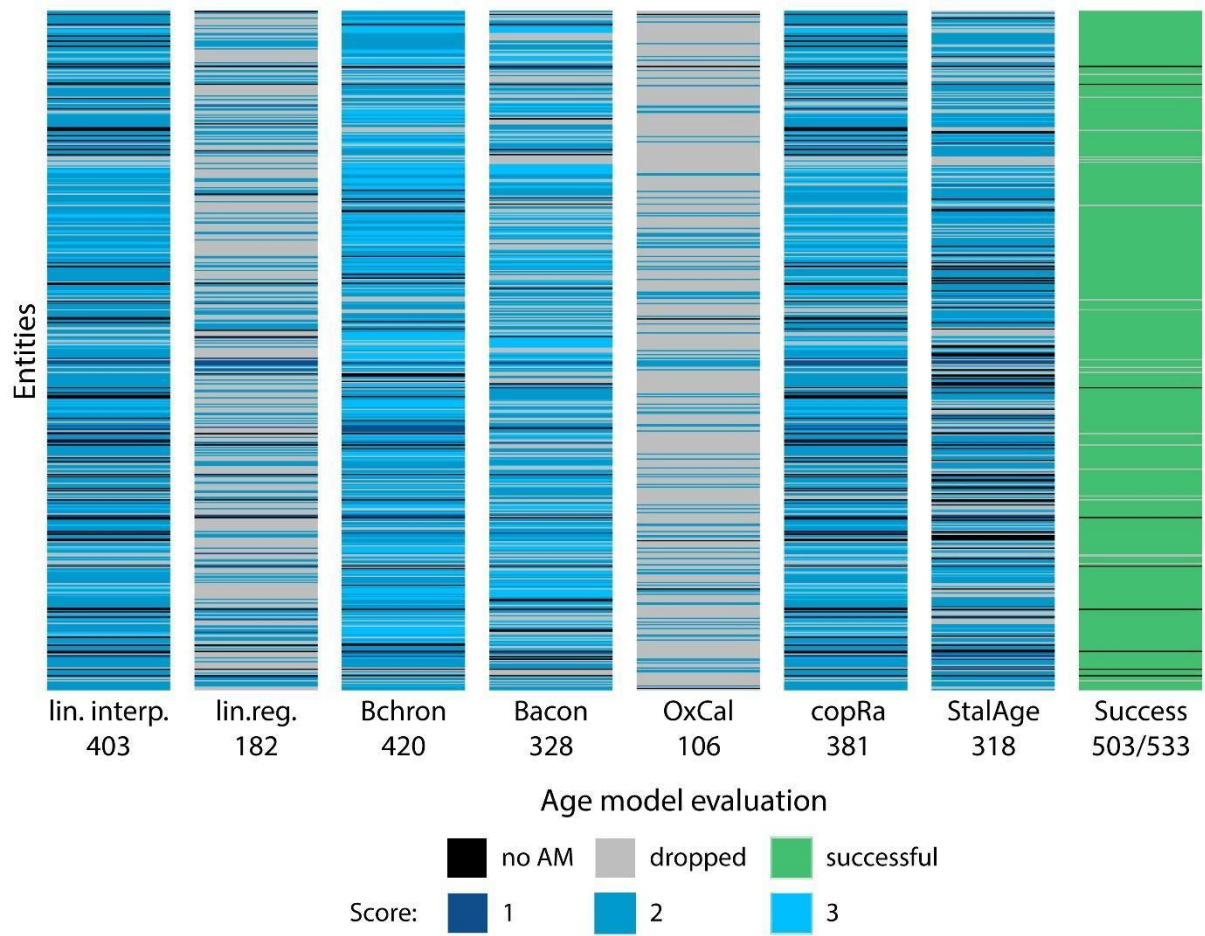


425
426

427 **Figure 4:** Visual summary of quality control of the automated SISAL chronology construction.
428 The evaluation of the age-depth models for each method (x-axis) is given for each entity (y-axis)
429 that was considered for the construction (n=533). Black lines mark age-depth models that could
430 not be computed. Age-depth models dropped in the automated or expert evaluation are
431 marked by grey lines. Age-depth models retained in SISALv2 are scored from 1 (only one
432 criterion satisfied) to 3 (all criteria satisfied) in shades of blue. For ~~504~~503 records alternative
433 age-depth models with uncertainties are provided (green lines) in the “success” column.

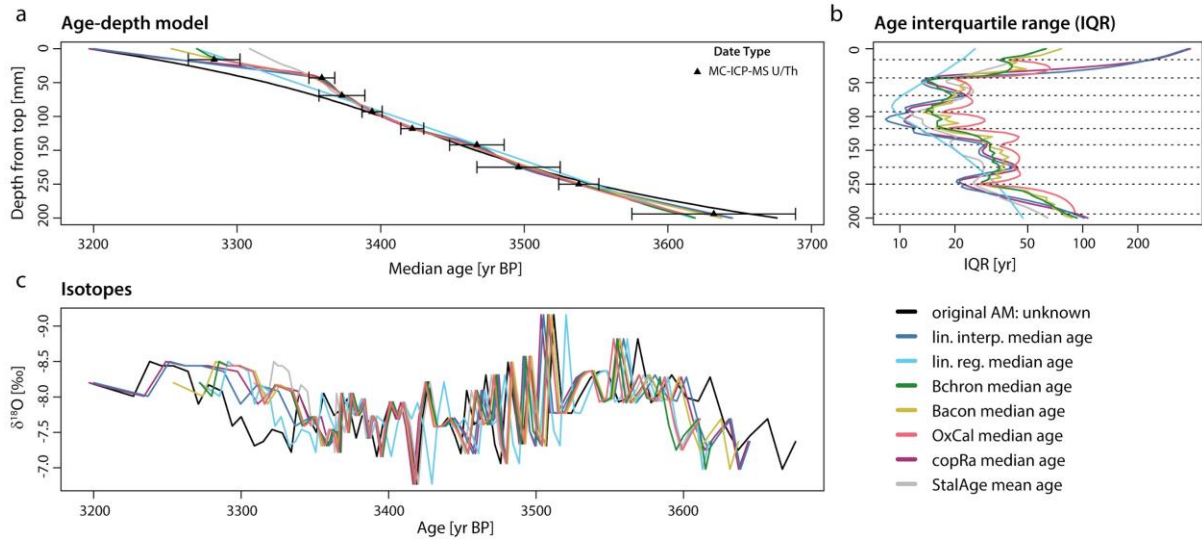


434



435

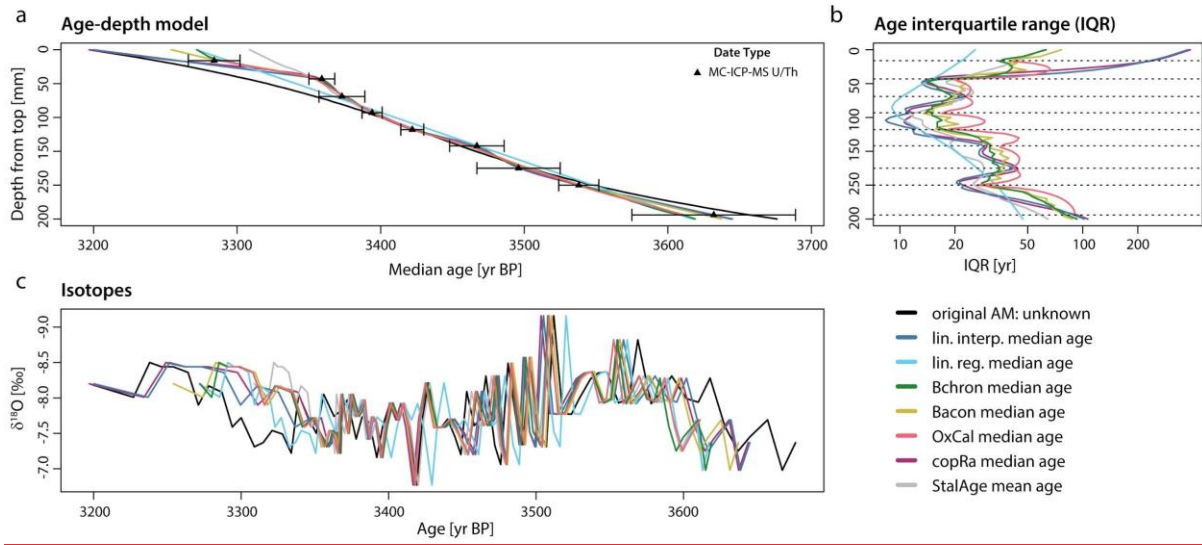
436 **Figure 5:** Illustration of the impact of the age model choice on reconstructed speleothem
 437 chronology illustrated by the KNI-51-H speleothem record (entity_id 342; Denniston et al.,
 438 2013b). Panel (a) shows the median and mean age estimates for each downcore sample from
 439 the different age models; (b) shows the interquartile range (IQR) of the ages. Horizontal dashed
 440 lines show the depths of the measured dates; (c) shows the isotopic record using the different
 441 age models.



442
 443

444

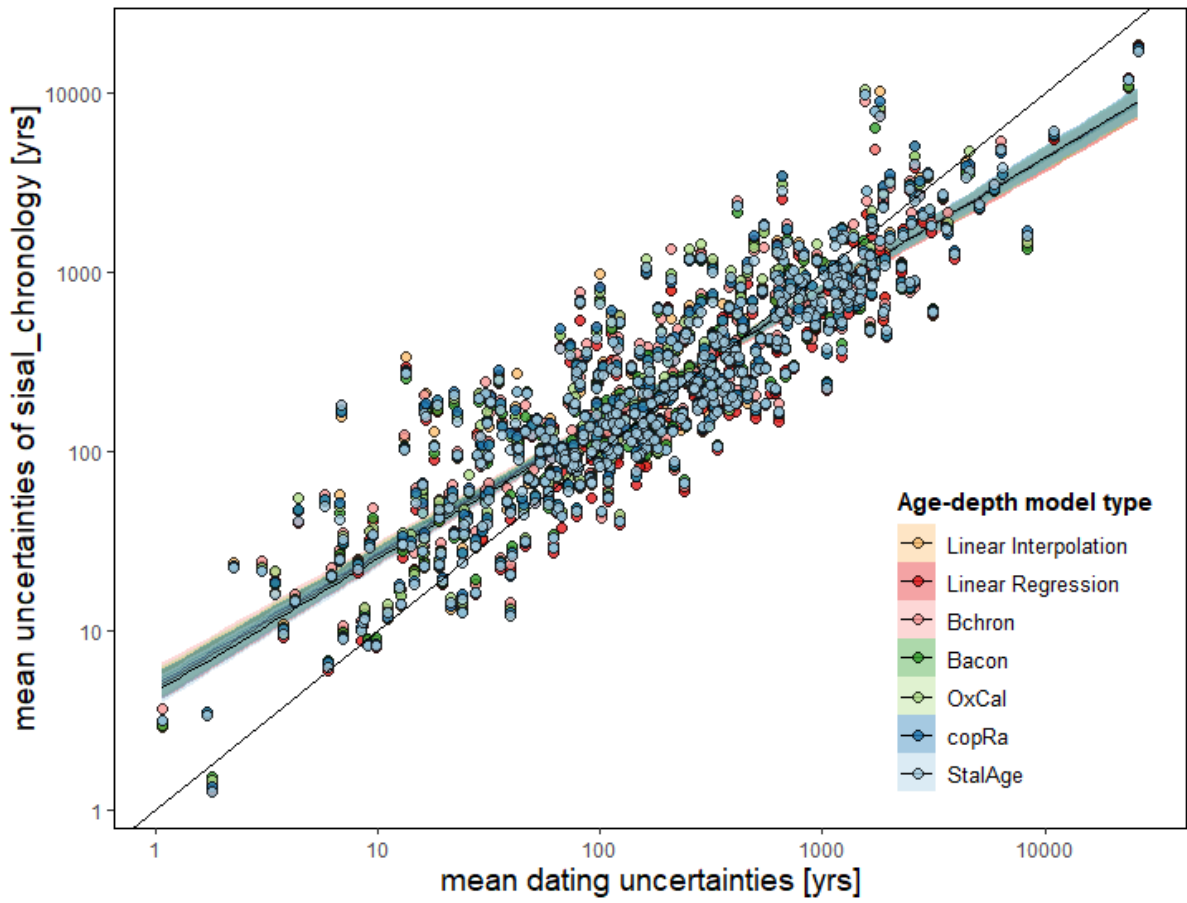
Figure 6



445

446

447 **Figure 6:** Scatter plot of average uncertainties in the sisal chronology table and U/Th mean
448 dating uncertainties for each entity and age-depth model technique. The 1:1 line is shown in
449 black.

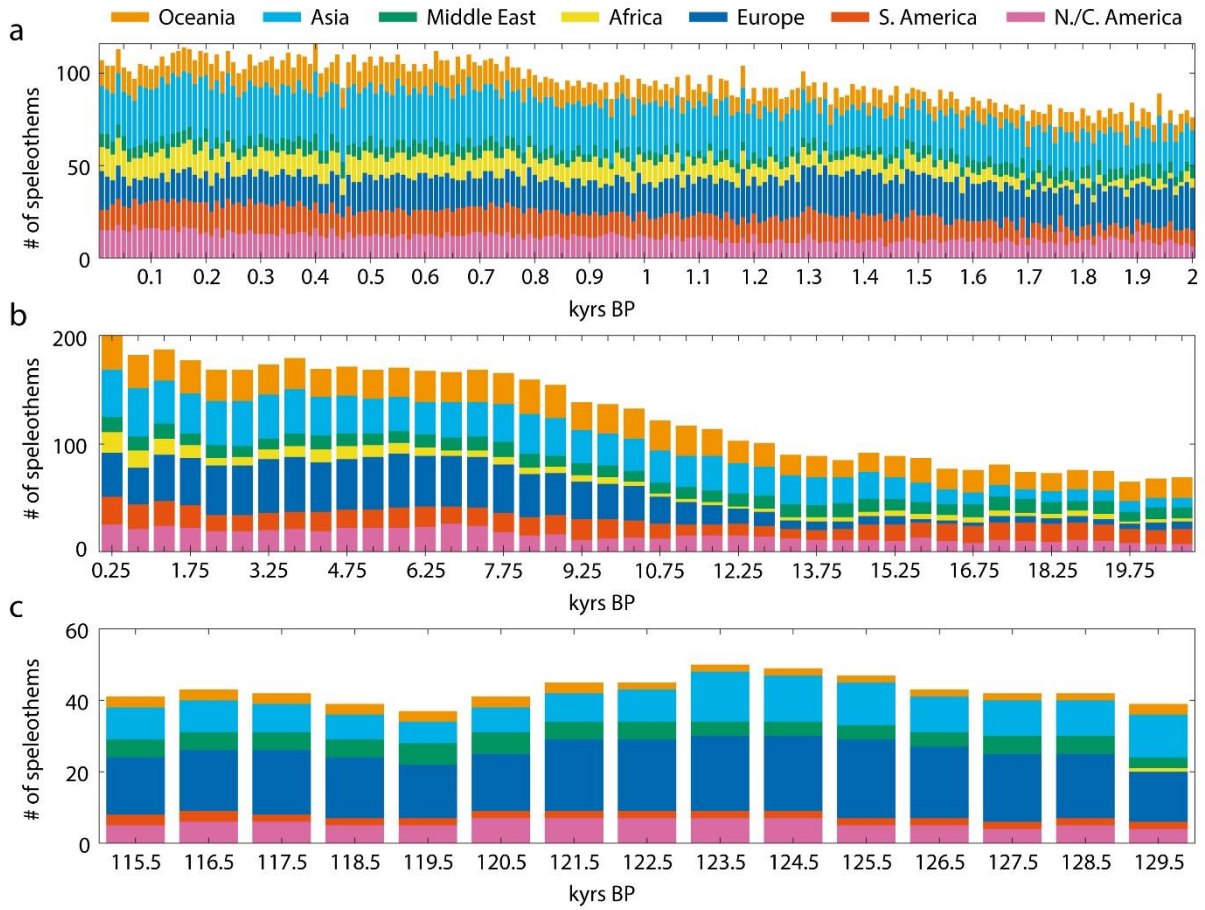


450
451

452 **Figure 7:** Global and regional temporal coverage of entities in the SISALv2. (a) last 2,000 years
 453 with a bin size of 10 years; (b) last 21,000 years with a bin size of 500 years; (c) the period between
 454 115,000 and 130,000 years BP with a bin size of 1,000 yrs. BP refers to “Before Present” where
 455 present is 1950 CE. Regions defined as in Table 7.



456



457
458

459 **Table 1:** Details of the `sisal_chronology` table. All ages in SISAL are reported as years BP (Before
460 Present) where present is 1950 CE.
461

Field label	Description	Format	Constraints
<i>sample_id</i>	Refers to the unique identifier for the sample (as given in the sample table)	Numeric	Positive integer
<i>lin_interp_age</i>	Age of the sample in years calculated with linear interpolation between dates	Numeric	None
<i>lin_interp_age_uncert_pos</i>	Positive 2-sigma uncertainty of the age of the sample in years calculated with linear interpolation between dates	Numeric	Positive decimal
<i>lin_interp_age_uncert_neg</i>	Negative 2-sigma uncertainty of the age of the sample in years calculated with linear interpolation between dates	Numeric	Positive decimal
<i>lin_reg_age</i>	Age of the sample in years calculated with linear regression	Numeric	None
<i>lin_reg_age_uncert_pos</i>	Positive 2-sigma uncertainty of the age of the sample in years calculated with linear regression	Numeric	Positive decimal
<i>lin_reg_age_uncert_neg</i>	Negative 2-sigma uncertainty of the age of the sample in years calculated with linear regression	Numeric	Positive decimal
<i>Bchron_age</i>	Age of the sample in years calculated with Bchron	Numeric	None
<i>Bchron_age_uncert_pos</i>	Positive 2-sigma uncertainty of the age of the sample in years calculated with Bchron	Numeric	Positive decimal
<i>Bchron_age_uncert_neg</i>	Negative 2-sigma uncertainty of the age of the sample in years calculated with Bchron	Numeric	Positive decimal
<i>Bacon_age</i>	Age of the sample in years calculated with Bacon	Numeric	None
<i>Bacon_age_uncert_pos</i>	Positive 2-sigma uncertainty of the age of the sample in years calculated with Bacon	Numeric	Positive decimal
<i>Bacon_age_uncert_neg</i>	Negative 2-sigma uncertainty of the age of the sample in years calculated with Bacon	Numeric	Positive decimal
<i>OxCal_age</i>	Age of the sample in years calculated with OxCal	Numeric	None
<i>OxCal_age_uncert_pos</i>	Positive 2-sigma uncertainty of the age of the sample in years calculated with OxCal	Numeric	Positive decimal
<i>OxCal_age_uncert_neg</i>	Negative 2-sigma uncertainty of the age of the sample in years calculated with OxCal	Numeric	Positive decimal
<i>copRa_age</i>	Age of the sample in years calculated with copRa	Numeric	None

<i>copRa_age_uncert_pos</i>	Positive 2-sigma uncertainty of the age of the sample in years calculated with copRa	Numeric	Positive decimal
<i>copRa_age_uncert_neg</i>	Negative 2-sigma uncertainty of the age of the sample in years calculated with copRa	Numeric	Positive decimal
<i>Stalage_age</i>	Age of the sample in years calculated with StalAge	Numeric	None
<i>Stalage_age_uncert_pos</i>	Positive 2-sigma uncertainty of the age of the sample in years calculated with StalAge	Numeric	Positive decimal
<i>Stalage_age_uncert_neg</i>	Negative 2-sigma uncertainty of the age of the sample in years calculated with StalAge	Numeric	Positive decimal

462

463 **Table 2:** Changes made to the Dating table to accommodate the new age models. These
464 changes are marked with (*) in Figure 2.

465

Action	Field label	Description	Format	Constraints
Field added	<i>date_used_lin_age</i>	Indication whether that date was used to construct the linear age model	Text	Selected from pre-defined list: "yes", "no".
Field added	<i>date_used_lin_reg</i>	Indication whether that date was used to construct the age model based on linear regression	Text	Selected from pre-defined list: "yes", "no".
Field added	<i>date_used_Bchron</i>	Indication whether that date was used to construct the age model based on Bchron	Text	Selected from pre-defined list: "yes", "no".
Field added	<i>date_used_Bacon</i>	Indication whether that date was used to construct the age model based on Bacon	Text	Selected from pre-defined list: "yes", "no".
Field added	<i>date_used_OxCal</i>	Indication whether that date was used to construct the age model based on OxCal	Text	Selected from pre-defined list: "yes", "no".
Field added	<i>date_used_copRa</i>	Indication whether that date was used to construct the copRa-based age model	Text	Selected from pre-defined list: "yes", "no".
Field added	<i>date_used_StalAge</i>	Indication whether that date was used to construct the age model based on StalAge	Text	Selected from pre-defined list: "yes", "no".

466

467

468 **Table 3:** Changes made to tables other than the *sisal_chronology* since the publication of SISALv1
 469 (Atsawawaranunt et al., 2018a; Atsawawaranunt et al., 2018b).

Table name	Action	Field label	Reason	Format	Constraints
Dating	Removed “sampling gap” option	<i>date_type</i>	This option was never used	Text	Selected from pre-defined list
	“others” option changed to “other”	<i>decay_constant</i>	Correction of typo	Text	Selected from pre-defined list
	Added “other” option	<i>calib_used</i>	Option added to accommodate new entities	Text	Selected from pre-defined list
	Added “other” option	<i>date_type</i>	Option added to accommodate new entities	Text	Selected from pre-defined list
Sample	Added “other” option	<i>original_chronology</i>	Option added to accommodate new entities	Text	Selected from pre-defined list
	Added “other” option	<i>ann_lam_check</i>	Option added to accommodate new entities	Text	Selected from pre-defined list

470

471 **Table 4:** Summary of the modifications applied to records already in version 1 (Atsawawaranunt
 472 et al., 2018b) and version 1b (Atsawawaranunt et al., 2019) of the SISAL database. Mistakes in
 473 previous versions of the database were identified as outlined in the Supplementary material and
 474 through analysing the data for the SISAL publications.

475

Modification	V1 to v1b	V1b to v2
Site table		
Number of new sites	37	82
Sites with new entities	11	32
Sites with altered site.site_name altered	3	15
Sites with changes in site.latitude	4	29
Sites with changes in site.longitude	6	32
Sites with changes in site.elevation	13	11
Sites with site.geology updated	7	6
Sites with site.rock_age info updated	3	8
Sites with site.monitoring info updated	0	13
Entity table		
Number of new entities	74	236
How many entities were added to pre-existing sites?	17	84
Entities with revised entity_name	2	25
Entities with updated entity.entity_status	1	10

Entities with altered entity.corresponding current	0	11
Entities with altered entity.depth_ref?	0	1
Entities with altered entity.cover_thickness	1	3
Entities with altered entity.distance_entrance	0	3
Entities with revised entity. speleothem_type	14	4
Entities with revised entity.drip_type	10	2
Entities with altered entity.d13C	1	0
Entities with altered entity.d18O	1	0
Entities with altered entity.d18O_water_equilibrium	4	6
Entities with altered entity.trace_elements	1	2
Entities with altered entity.organics	1	2
Entities with altered entity.fluid_inclusions	1	3
Entities with altered entity.mineralogy_petrology_fabric	1	2
Entities with altered entity.clumped_isotopes	1	3
Entities with altered entity.noble_gas_temperatures	1	2
Entities with altered entity.C14	1	2
Entities with altered entity.ODL	1	2
Entities with altered entity.Mg_Ca	1	2
Entities with altered entity.contact (mostly correction of typos)	7	32
Entities with altered entity.Data_DOI_URL (revision mostly to permanent links)	134	14
Dating table		
Entities with changes in the dating table	70	260 269
Addition of "Event: hiatus" to an entity	0	3
How many hiatuses had their depth changed?	2	7
Entities with the depths of "Event: start/end of laminations" changed.	0	5
Entities with altered dating.date_type	11	30
Entities with altered dating.depth_dating	14	45
Entities with altered dating.dating_thickness	14	37
Entities with altered dating.material_dated	5	62
Entities with altered dating.min_weight	13	56
Entities with altered dating.max_weight	19	36
Entities with altered dating.uncorr_age	18	48
Entities with altered dating.uncorr_age_uncert_pos	12	53
Entities with altered dating.uncorr_age_uncert_neg	12	41 40
Entities with altered dating.14C_correction	17	36
Entities with altered dating.calib_used	13	32
Entities with altered dating.date_used	4	51
Entities with altered dating.238U_content	11	45 47
Entities with altered dating.238U_uncertainty	16	28 29
Entities with altered dating.232Th_content	15	46
Entities with altered dating.232Th_uncertainty	14	50
Entities with altered dating.230Th_content	11	40
Entities with altered dating.230Th_uncertainty	15	38
Entities with altered dating.230Th_232Th_ratio	5	59 60
Entities with altered dating.230Th_232Th_ratio_uncertainty	14	48 49
Entities with altered dating.230Th_238U_activity	19	39 40

Entities with altered dating.230Th_238U_activity_uncertainty	17	4449
Entities with altered dating.234U_238U_activity	12	5140
Entities with altered dating.234U_238U_activity_uncertainty	11	4840
Entities with altered dating.ini_230Th_232Th_ratio	15	5941
Entities with altered dating.ini_230Th_232Th_ratio_uncertainty	8	6049
Entities with altered dating.decay_constant	17	55
Entities with altered dating.corr_age	17	3536
Entities with altered dating.corr_age_uncert_pos	13	4647
Entities with altered dating.corr_age_uncert_neg	9	4752
Sample table		
Altered sample.depth_sample	0	15
Altered sample.mineralogy	0	20
Altered sample.arag_corr	11	20
How many entities had their d18O time-series altered (i.e. changes in depth and/or isotope values as in duplicates)?	13	9596
How many entities had their d13C time-series altered (i.e. changes in depth and/or isotope values as in duplicates)?	8	64
Original chronology		
Entities with altered original_chronology.interp_age	1	42
Entities with altered original_chronology.interp_age_uncert_pos	0	14
Entities with altered original_chronology.interp_age_uncert_neg	0	14
References		
How many entities had their references changed (changes/additions/removals)?	6	16
How many citations have a different pub_Doi?	2	16
Notes		
Sites with notes removed	7	5
Sites with notes added	32	68
Sites with notes modified	21	3433

476
477
478
479
480

Table 5: Information on new speleothem records (entities) added to the SISAL_v2 database from SISALv1b (Comas-Bru et al., 2019). There may be multiple entities from a single cave, here identified as the site. Latitude (Lat) and Longitude (Lon) are given in decimal degrees North and East respectively.

Site_id	Site_name	Lat (N)	Lon (E)	Region	Entity_id	Entity_name	Reference
2	Kesang cave	42.87	81.75	China	620	CNKS-2	Cai et al. (2017)
					621	CNKS-3	Cai et al. (2017)
					622	CNKS-7	Cai et al. (2017)
					623	CNKS-9	Cai et al. (2017)
6	Hulu cave	32.5	119.17	China	617	MSP	Cheng et al. (2006)
					618	MSX	Cheng et al. (2006)

					619	MSH	Cheng et al. (2006)
12	Mawmluh cave	25.262 2	91.8817	India	476	ML.1	Kathayat et al. (2018)
					477	ML.2	Kathayat et al. (2018)
					495	KM-1	Huguet et al. (2018)
13	Ball Gown cave	-17.03	125	Australia	633	BGC-5	Denniston et al. (2013b); Denniston et al. (2017a)
					634	BGC-10	Denniston et al. (2013b); Denniston et al. (2017a)
					635	BGC-11_2017	Denniston et al. (2013b); Denniston et al. (2017a)
					636	BGC-16	Denniston et al. (2013b); Denniston et al. (2017a)
14	Lehman caves	39.01	-114.22	United States	641	CDR3	Steponaitis et al. (2015)
					642	WR11	Steponaitis et al. (2015)
15	Baschg cave	47.250 1	9.6667	Austria	643	BA-5	Moseley et al. (2019)
					644	BA-7	Moseley et al. (2019)
23	Lapa grande cave	-14.37	-44.28	Brazil	614	LG12B	Stríkis et al. (2018)
					615	LG10	Stríkis et al. (2018)
					616	LG25	Stríkis et al. (2018)
24	Lapa sem fim cave	- 16.150 3	-44.6281	Brazil	603	LSF15	Stríkis et al. (2018)
					604	LSF3_2018	Stríkis et al. (2018)
					605	LSF13	Stríkis et al. (2018)
					606	LSF11	Stríkis et al. (2018)
					607	LSF9	Stríkis et al. (2018)
27	Tamboril cave	-16	-47	Brazil	594	TM6	Ward et al. (2019)
39	Dongge cave	25.283 3	108.0833	China	475	DA_2009	Cheng et al. (2009)
54	Sahiya cave	30.6	77.8667	India	478	SAH-2	Kathayat et al. (2017)

					479	SAH-3	Kathayat et al. (2017)
					480	SAH-6	Kathayat et al. (2017)
65	Whiterock cave	4.15	114.86	Malaysia (Borneo)	685	WR12-01	Carolyn et al. (2016)
					686	WR12-12	Carolyn et al. (2016)
72	Ascunsa cave	45	22.6	Romania	582	POM1	Staubwasser et al. (2018)
82	Hollywood cave	-41.95	171.47	New Zealand	673	HW-1	Williams et al. (2005)
86	Modric cave	44.2568	15.5372	Croatia	631	MOD-27	Rudzka-Phillips et al. (2013)
					632	MOD-21	Rudzka et al. (2012)
105	Schneckenloch cave	47.4333	9.8667	Austria	663	SCH-6	Moseley et al. (2019)
113	Paixao cave	-12.6182	-41.0184	Brazil	611	PX5	Strikis et al. (2015)
					612	PX7_2018	Strikis et al. (2018)
115	Hölloch im Mahdtal	47.3781	10.1506	Germany	664	HOL-19	Moseley et al. (2019)
117	Bunker cave	51.3675	7.6647	Germany	596	Bu2_2018	Weber et al. (2018)
128	Buckeye creek	37.98	-80.4	United States	681	BCC-9	Cheng et al. (2019)
					682	BCC-10_2019	Cheng et al. (2019)
					683	BCC-30	Cheng et al. (2019)
135	Grotte de Piste	33.95	-4.246	Morocco	464	GP5	Ait Brahim et al. (2018)
					591	GP2	Ait Brahim et al. (2018)
138	Moomi cave	12.55	54.2	Yemen (Socotra)	481	M1-2	Mangini, Cheng et al. (unpublished); Burns et al. (2003); Burns et al. (2004)
140	Sanbao cave	31.667	110.4333	China	482	SB3	Wang et al. (2008)
					483	SB-10_2008	Wang et al. (2008)
					484	SB11	Wang et al. (2008)
					485	SB22	Wang et al. (2008)
					486	SB23	Wang et al. (2008)
					487	SB24	Wang et al. (2008)

					488	SB25-1	Wang et al. (2008)
					489	SB25-2	Wang et al. (2008)
					490	SB-26_2008	Wang et al. (2008)
					491	SB34	Wang et al. (2008)
					492	SB41	Wang et al. (2008)
					493	SB42	Wang et al. (2008)
					494	TF	Wang et al. (2008)
141	Sofular cave	41.4167	31.9333	Turkey	456	SO-2	Badertscher et al. (2011) Fleitmann et al. (2009); Göktürk et al. (2011)
					687	SO-4	Badertscher et al. (2011)
					688	SO-6	Badertscher et al. (2011)
					689	SO-14B	Badertscher et al. (2011)
145	Antro del Corchia	43.9833	10.2167	Italy	665	CC-1_2018	Tzedakis et al. (2018)
					666	CC-5_2018	Tzedakis et al. (2018)
					667	CC-7_2018	Tzedakis et al. (2018)
					668	CC-28_2018	Tzedakis et al. (2018)
					669	CC_stack	Tzedakis et al. (2018)
					670	CC27	Isola et al. (2019)
155	KNI-51	-15.3	128.62	Australia	637	KNI-51-1	Denniston et al. (2017a)
					638	KNI-51-8	Denniston et al. (2017a)
160	Soreq cave	31.7558	35.0226	Israel	690	Soreq-composite185	Bar-Matthews et al. (2003)
165	Ruakuri cave	-36.27	175.08	New Zealand	674	RK-A	Williams et al. (2010)
165	Ruakuri cave	-36.27	175.08	New Zealand	675	RK-B	Williams et al. (2010)
165	Ruakuri cave	-36.27	175.08	New Zealand	676	RK05-1	Whittaker (2008)
165	Ruakuri cave	-36.27	175.08	New Zealand	677	RK05-3	Whittaker (2008)
165	Ruakuri cave	-36.27	175.08	New Zealand	678	RK05-4	Whittaker (2008)

177	Santo Tomas cave	22.55	-83.84	Cuba	608	CM_2019	Warken et al. (2019)
					609	CMa	Warken et al. (2019)
					610	CMb	Warken et al. (2019)
179	Closani Cave	45.10	22.8	Romania	390	C09-2	Warken et al. (2018)
182	Kotumsar cave	19	82	India	590	KOT-I	Band et al. (2018)
192	El Condor cave	-5.93	-77.3	Peru	592	ELC-A	Cheng et al. (2013)
					593	ELC-B	Cheng et al. (2013)
198	Lianhua cave, Hunan	29.48	109.5333	China	496	LH-2	Zhang et al. (2013)
213	Tausoare cave	47.4333	24.5167	Romania	457	1152	Staubwasser et al. (2018)
214	Cave C126	-22.1	113.9	Australia	458	C126-117	Denniston et al. (2013a)
					459	C126-118	Denniston et al. (2013a)
215	Chacara cave	33.9558	-4.2461	Morocco	460	Cha2_2018	Ait Brahim et al. (2018)
					588	Cha2_2019	Ait Brahim et al. (2019)
					589	Cha1	Ait Brahim et al. (2019)
216	Dark cave	27.2	106.1667	China	461	D1	Jiang et al. (2013)
					462	D2	Jiang et al. (2013)
217	E'mei cave	29.5	115.5	China	463	EM1	Zhang et al. (2018b)
218	Nuanhe cave	41.3333	124.9167	China	465	NH6	Wu et al. (2012)
					466	NH33	Wu et al. (2012)
219	Shennong cave	28.71	117.26	China	467	SN17	Zhang et al. (2018a)
220	Baeg-nyong cave	37.27	128.58	South Korea	468	BN-1	Jo et al. (2017)
221	La Vierge cave	-19.7572	63.3703	Rodrigues	469	LAVI-4	Li et al. (2018)
222	Patate cave	-19.7583	63.3864	Rodrigues	470	PATA-1	Li et al. (2018)
223	Wanxiang cave	33.32	105	China	471	WX42B	Zhang et al. (2008)
					679	WXSM-51	Johnson et al. (2006)
					680	WXSM-52	Johnson et al. (2006)

224	Xianglong cave	33	106.33	China	472	XL16	Tan et al. (2018a)
					473	XL2	Tan et al. (2018a)
					474	XL26	Tan et al. (2018a)
225	Chiflonkhakha cave	-18.1222	-65.7739	Bolivia	497	Boto 1	Apaestegui et al. (2018)
					498	Boto 3	Apaestegui et al. (2018)
					499	Boto 7	Apaestegui et al. (2018)
226	Cueva del Diamante	-5.73	-77.5	Peru	500	NAR-C	Cheng et al. (2013)
					501	NAR-C-D	Cheng et al. (2013)
					502	NAR-C-F	Cheng et al. (2013)
					503	NAR-D	Cheng et al. (2013)
					504	NAR-F	Cheng et al. (2013)
227	El Capitan cave	56.162	-133.319	United States	505	EC-16-5-F	Wilcox et al. (2019)
228	Bat cave	32.1	-104.26	United States	506	BC-11	Asmerom et al. (2013)
229	Actun Tunichil Muknal	17.1	-88.85	Belize	507	ATM-7	Frappier et al. (2002); Frappier et al. (2007); Jamieson et al. (2015)
230	Marota cave	-12.6227	-41.0216	Brazil	508	MAG	Stríkis et al. (2018)
231	Pacupahuain cave	-11.24	-75.82	Peru	509	P09PH2	Kanner et al. (2012)
232	Rio Secreto cave system	20.59	-87.13	Mexico	510	Itzamna	Medina-Elizalde et al., (2016); Medina-Elizalde et al. (2017)
233	Robinson cave	33	-107.7	United States	511	KR1	Polyak et al. (2017)
234	Santana cave	-24.5308	-48.7267	Brazil	512	St8-a	Cruz et al. (2006)
					513	St8-b	Cruz et al. (2006)
235	Cueva del Tigre Perdido	-5.9406	-77.3081	Peru	514	NC-A	van Breukelen et al. (2008)
					515	NC-B	van Breukelen et al. (2008)

236	Toca da Boa Vista	-10.1602	-40.8605	Brazil	516	TBV40	Wendt et al. (2019)
					517	TBV63	Wendt et al. (2019)
237	Umajalanta cave	-18.12	-65.77	Bolivia	518	Boto 10	Apaeategui et al. (2018)
238	Akalagavi cave	14.9833	74.5167	India	519	MGY	Yadava et al. (2004)
239	Baluk cave	42.433	84.733	China	520	BLK12B	Liu et al. (2019)
240	Baratang cave	12.0833	92.75	India	521	AN4	Laskar et al. (2013)
					522	AN8	Laskar et al. (2013)
241	Gempa bumi cave	-5	120	Indonesia (Sulawesi)	523	GB09-03	Krause et al. (2019)
					524	GB11-09	Krause et al. (2019)
242	Haozhu cave	30.6833	109.9833	China	525	HZZ-11	Zhang et al. (2016)
					526	HZZ-27	Zhang et al. (2016)
243	Kailash cave	18.8445	81.9915	India	527	KG-6	Gautam et al. (2019)
244	Lianhua cave, Shanxi	38.1667	113.7167	China	528	LH1	Dong et al. (2018)
					529	LH4	Dong et al. (2018)
					530	LH5	Dong et al. (2018)
					531	LH6	Dong et al. (2018)
					532	LH9	Dong et al. (2018)
					533	LH30	Dong et al. (2018)
245	Nakarallu cave	14.52	77.99	India	534	NK-1305	Sinha et al. (2018)
246	Palawan cave	10.2	118.9	Malaysia (Northern Borneo)	535	SR02	Partin et al. (2015)
247	Shalaih cave	35.1469	45.2958	Iraq	536	SHC-01	Marsh et al. (2018); Amin Al-Manmi et al. (2019)
					537	SHC-02	Marsh et al. (2018); Amin Al-Manmi et al. (2019)
248	Shenqi cave	28.333	103.1	China	538	SQ1	Tan et al. (2018b)
					539	SQ7	Tan et al. (2018b)

249	Shigao cave	28.183	107.167	China	540	SG1	Jiang et al. (2012)
					541	SG2	Jiang et al. (2012)
250	Wuya cave	33.82	105.43	China	542	WY27	Tan et al. (2015)
					543	WY33	Tan et al. (2015)
251	Zhenzhu cave	38.25	113.7	China	544	ZZ12	Yin et al. (2017)
252	Andriamanilok e	- 24.051	43.7569	Madagascar	545	AD4	Scropton et al. (2019)
253	Hoq cave	12.5866	54.3543	Yemen (Socotra)	546	Hq-1	Van Rempelbergh et al. (2013)
					547	STM1	Van Rempelbergh et al. (2013)
					548	STM6	Van Rempelbergh et al. (2013)
254	PP29	- 34.2078	22.0876	South Africa	549	46745	Braun et al. (2019b)
					550	46746-a	Braun et al. (2019b)
					551	46747	Braun et al. (2019b)
					552	138862.1	Braun et al. (2019b)
					553	138862.2a	Braun et al. (2019b)
					554	142828	Braun et al. (2019b)
					555	46746-b	Braun et al. (2019b)
					556	138862.2b	Braun et al. (2019b)
255	Mitoho	- 24.0477	43.7533	Madagascar	557	MT1	Scropton et al. (2019)
256	Lithophagus cave	46.828	22.6	Romania	558	LFG-2	Lauritzen and Onac (1999)
257	Akcakale cave	40.4498	39.5365	Turkey	559	2p	Jex et al. (2010); Jex et al. (2011); Jex et al. (2013)
258	B7 cave	49	7	Germany	560	STAL-B7-7	Niggemann et al. (2003b)
259	Cobre cave	42.98	-4.37	Spain	561	PA-8	Osete et al. (2012); Rossi et al. (2014)
260	Crovassa Azzurra	39.28	8.48	Italy	562	CA	Columbu et al. (2019)
261	El Soplao cave	43.2962	-4.3937	Spain	563	SIR-1	Rossi et al. (2018)

262	Bleßberg cave	50.424 4	11.0203	Germany	564	BB-1	Breitenbach et al. (2019)
					565	BB-3	Breitenbach et al. (2019)
263	Orlova Chuka cave	43.593 7	25.9597	Bulgaria	566	ocz-6	Pawlak et al. (2019)
264	Strašna peć cave	44.004 9	15.0388	Croatia	567	SPD-1	Lončar et al. (2019)
					568	SPD-2	Lončar et al. (2019)
265	Coves de Campanet	39.793 7	2.9683	Spain	569	CAM-1	Dumitru et al. (2018)
266	Cueva Victoria	37.632 2	-0.8215	Spain	570	Vic-III-4	Budsky et al. (2019)
267	Gruta do Casal da Lebre	39.3	-9.2667	Portugal	571	GCL6	Denniston et al. (2017b)
268	Pere Noel cave	50	5.2	Belgium	572	PN-95-5	Verheyden et al. (2000); Verheyden et al. (2014)
269	Gejkar cave	35.8	45.1645	Iraq	573	Gej-1	Flohr et al. (2017)
270	Gol-E-Zard cave	35.84	52	Iran	574	GZ14-1	Carolin et al. (2019)
271	Jersey cave	-35.72	148.49	Australia	575	YB-F1	Webb et al. (2014)
272	Metro cave	-41.93	171.47	New Zealand	576	M-1	Logan (2011)
273	Crystal cave	36.59	-118.82	United States	577	CRC-3	McCabe-Glynn et al. (2013)
274	Terciopelo cave	10.17	-85.33	Costa Rica	578	CT-1	Lachniet et al. (2009)
					579	CT-5	Lachniet et al. (2009)
					580	CT-6	Lachniet et al. (2009)
					581	CT-7	Lachniet et al. (2009)
275	Buraca Gloriosa	39.533 3	-8.7833	Portugal	583	BG41	Denniston et al. (2017b)
					584	BG66	Denniston et al. (2017b)
					585	BG67	Denniston et al. (2017b)
					586	BG611	Denniston et al. (2017b)
					587	BG6LR	Denniston et al. (2017b)
276	Béke cave	48.483 3	20.5167	Hungary	595	BNT-2	Demény et al. (2019)
							Czuppon et al. (2018)
277	Huagapo cave	-11.27	-75.79	Peru	597	P00-H2	Kanner et al. (2013)

					598	P00-H1	Kanner et al. (2013)
					599	P09-H1b	Burns et al. (2019)
					600	P10-H5	Burns et al. (2019)
					601	P10-H2	Burns et al. (2019)
					602	PeruMIS6Composite	Burns et al. (2019)
278	Pink Panther cave	32	-105.2	United States	613	PP1	Asmerom et al. (2007)
279	Staircase cave	-34.2071	22.0899	South Africa	624	46322	Braun et al. (2019b)
					625	46330-a	Braun et al. (2019b)
					626	46861	Braun et al. (2019b)
					627	50100	Braun et al. (2019b)
					628	142819	Braun et al. (2019b)
					629	142820	Braun et al. (2019b)
					630	46330-b	Braun et al. (2019b)
280	Atta cave	51.1	7.9	Germany	639	AH-1	Niggemann et al. (2003a)
281	Venado cave	10.55	-84.77	Costa Rica	640	V1	Lachniet et al. (2004)
282	Wadi Sannur cave	28.6167	31.2833	Egypt	691	WS-5d	El-Shenawy et al. (2018)
283	Babylon cave	-41.95	171.47	New Zealand	645	BN-1	Williams et al. (2005)
					646	BN-2	Williams et al. (2005)
					647	BN-3	P. Williams et al., unpublished
284	Creighton's cave	-40.63	172.47	New Zealand	648	CN-1	Williams et al. (2005)
285	Disbelief cave	-38.82	177.52	New Zealand	649	Disbelief	Lorrey et al. (2008)
286	La Garma cave	43.4306	-3.6658	Spain	650	GAR-01_drill	Baldini et al. (2015); Baldini et al. (2019)
					651	GAR-01_laser_d180	Baldini et al. (2015)
					652	GAR-01_laser_d13C	Baldini et al. (2015)
287	Twin Forks cave	-40.63	172.48	New Zealand	653	TF-2	Williams et al. (2005)
288	Wet Neck cave	-40.7	172.48	New Zealand	654	WN-4	Williams et al. (2005)

					655	WN-11	Williams et al. (2005)
289	Gassel Tropfsteinhöhle	47.8228	13.8428	Austria	656	GAS-12	Moseley et al. (2019)
					657	GAS-13	Moseley et al. (2019)
					658	GAS-22	Moseley et al. (2019)
					659	GAS-25	Moseley et al. (2019)
					660	GAS-27	Moseley et al. (2019)
					661	GAS-29	Moseley et al. (2019)
290	Grete-Ruth Shaft	47.5429	12.0272	Austria	662	HUN-14	Moseley et al. (2019)
292	Limnon cave	37.9605	22.1403	Greece	671	KTR-2	Peckover et al. (2019)
293	Tham Doun Mai	20.75	102.65	Laos	672	TM-17	Wang et al. (2019)
294	Palco cave	18.35	-66.5	Puerto Rico	684	PA-2b	Rivera-Collazo et al. (2015)
179	Closani Cave	45.10	22.8	Romania	390	C09-2	Warken et al. (2018)

481

482 **Table 6:** Percentage of entities uploaded to the different versions of the SISAL database with
 483 respect to the number of records identified by the SISAL working group as of November 2019.
 484 The number of identified records includes potentially superseded speleothem records. Regions
 485 are defined as: Oceania ($-60^{\circ} < \text{Lat} < 0^{\circ}$; $90^{\circ} < \text{Lon} < 180^{\circ}$); Asia ($0^{\circ} < \text{Lat} < 60^{\circ}$; $60^{\circ} < \text{Lon} < 130^{\circ}$);
 486 Middle East ($7.6^{\circ} < \text{Lat} < 50^{\circ}$; $26^{\circ} < \text{Lon} < 59^{\circ}$); Africa ($-45^{\circ} < \text{Lat} < 36.1^{\circ}$; $-30^{\circ} < \text{Lon} < 60^{\circ}$; with
 487 records in the Middle East region removed); Europe ($36.7^{\circ} < \text{Lat} < 75^{\circ}$; $-30^{\circ} < \text{Lon} < 30^{\circ}$; plus
 488 Gibraltar and Siberian sites); South America (S. Am; $-60^{\circ} < \text{Lat} < 8^{\circ}$; $-150^{\circ} < \text{Lon} < -30^{\circ}$); North and
 489 Central America (N./C. Am; $8.1^{\circ} < \text{Lat} < 60^{\circ}$; $-150^{\circ} < \text{Lon} < -50^{\circ}$)
 490

Region	Version 1		Version 1b		Version 2	
	Entities	Sites	Entities	Sites	Entities	Sites
Oceania	47.7	36.7	56.8	51.0	80.2	69.4
Asia	36.2	28.8	41.1	33.3	64.8	48.5
Middle East	21.2	31.1	28.8	35.6	42.3	48.9
Africa	63.2	62.5	63.2	62.5	73.7	87.5
Europe	48.0	51.9	54.6	58.7	75.3	77.9
S. Am	30.6	39.5	40.8	50.0	77.6	73.7
N./C. Am	35.7	36.7	51.8	56.7	70.5	73.3

491

492 References

- 493 Ait Brahim, Y., Wassenburg, J. A., Cruz, F. W., Sifeddine, A., Scholz, D., Bouchaou, L., Dassie, E. P., Jochum,
494 K. P., Edwards, R. L., and Cheng, H.: Multi-decadal to centennial hydro-climate variability and linkage to
495 solar forcing in the Western Mediterranean during the last 1000 years, *Scientific Reports*, 8, 174466,
496 <https://doi.org/10.1038/s41598-018-35498-x>, 2018.
- 497 Ait Brahim, Y., Wassenburg, J. A., Sha, L., Cruz, F. W., Deininger, M., Sifeddine, A., Bouchaou, L., Spötl, C.,
498 Edwards, R. L., and Cheng, H.: North Atlantic Ice-Rafting, Ocean and Atmospheric Circulation During the
499 Holocene: Insights From Western Mediterranean Speleothems, *Geophysical Research Letters*, 46,
500 [2019GL082405-082019GL082405, GL082405](https://doi.org/10.1029/2019GL082405), <https://doi.org/10.1029/2019GL082405>, 2019.
- 501 Amin Al-Manmi, D. A. M., Ismaeel, S. B., and Altaweel, M.: Reconstruction of palaeoclimate in Shalaih Cave,
502 SE of Sangaw, Kurdistan Province of Iraq, *Palaeogeography, Palaeoclimatology, Palaeoecology*, 524, 262-
503 272, <https://doi.org/10.1016/j.palaeo.2019.03.044>, 2019.
- 504 [Amirnezhad-Mozhdehi, S., Comas-Bru, L. : MATLAB scripts to produce OxCal chronologies for SISAL](http://doi.org/10.5281/zenodo.3586280)
505 [database \(scripts V1\) \(Version 1.0\). Zenodo. http://doi.org/10.5281/zenodo.3586280, 2019.](http://doi.org/10.5281/zenodo.3586280)
- 506 Apaestegui, J., Cruz, F. W., Vuille, M., Fohlmeister, J., Espinoza, J. C., Sifeddine, A., Strikis, N., Guyot, J. L.,
507 Ventura, R., Cheng, H., and Edwards, R. L.: Precipitation changes over the eastern Bolivian Andes inferred
508 from speleothem (δ O-18) records for the last 1400 years, *Earth and Planetary Science Letters*, 494,
509 124-134, <https://doi.org/10.1016/j.epsl.2018.04.048>, 2018.
- 510 Asmerom, Y., Polyak, V., Burns, S., and Rasmussen, J.: Solar forcing of Holocene climate: New insights
511 from a speleothem record, southwestern United States, *Geology*, 35, 1-4,
512 <https://doi.org/10.1130/G22865A.1>, 2007.
- 513 Asmerom, Y., Polyak, V. J., Rasmussen, J. B. T., Burns, S. J., and Lachniet, M.: Multidecadal to multicentury
514 scale collapses of Northern Hemisphere monsoons over the past millennium, *Proceedings of the National*
515 *Academy of Sciences of the United States of America*, 110, 9651-9656,
516 [10.1073/pnas.1214870110](https://doi.org/10.1073/pnas.1214870110)<https://doi.org/10.1073/pnas.1214870110>, 2013.
- 517 Atsawawaranunt, K., Comas-Bru, L., Amirnezhad Mozhdehi, S., Deininger, M., Harrison, S. P., Baker, A.,
518 Boyd, M., Kaushal, N., Ahmad, S. M., Ait Brahim, Y., Arienzo, M., Bajo, P., Braun, K., Burstyn, Y., Chawchai,
519 S., Duan, W., Hatvani, I. G., Hu, J., Kern, Z., Labuhn, I., Lachniet, M., Lechleitner, F. A., Lorrey, A., Pérez-
520 Mejías, C., Pickering, R., Scroxton, N., and SISAL Working Group members, S. W. G.: The SISAL database: a
521 global resource to document oxygen and carbon isotope records from speleothems, *Earth System Science*
522 *Data*, 10, 1687-1713, <https://doi.org/10.5194/essd-10-1687-2018>, 2018a.
- 523 Atsawawaranunt, K., Harrison, S. and Comas-Bru, L.: SISAL (Speleothem Isotopes Synthesis and AnaLysis
524 Working Group) database Version 1.0. University of Reading. Dataset.:
525 <https://doi.org/10.17864/1947.147> 2018b.
- 526 Atsawawaranunt, K., Harrison, S. and Comas-Bru, L.: SISAL (Speleothem Isotopes Synthesis and AnaLysis
527 Working Group) database Version 1b. University of Reading. Dataset.:
528 <https://doi.org/10.17864/1947.189>, 2019.
- 529 Badertscher, S., Fleitmann, D., Cheng, H., Edwards, R. L., Göktürk, O. M., Zumbühl, A., Leuenberger, M.,
530 and Tüysüz, O.: Pleistocene water intrusions from the Mediterranean and Caspian seas into the Black Sea,
531 *Nature Geoscience*, 4, 236-239, <https://doi.org/10.1038/ngeo1106>, 2011.
- 532 Baldini, L. M., McDermott, F., Baldini, J. U. L., Arias, P., Cueto, M., Fairchild, I. J., Hoffmann, D. L., Matthey,
533 D. P., Muller, W., Nita, D. C., Ontanon, R., Garcia-Monco, C., and Richards, D. A.: Regional temperature,

- 534 atmospheric circulation, and sea-ice variability within the Younger Dryas Event constrained using a
535 speleothem from northern Iberia, *Earth and Planetary Science Letters*, 419, 101-110,
536 <https://doi.org/10.1016/j.epsl.2015.03.015>, 2015.
- 537 Baldini, L. M., Baldini, J. U. L., McDermott, F., Arias, P., Cueto, M., Fairchild, I. J., Hoffmann, D. L., Matthey,
538 D. P., Müller, W., Nita, D. C., Ontañón, R., Garcíá-Moncó, C., and Richards, D. A.: North Iberian temperature
539 and rainfall seasonality over the Younger Dryas and Holocene, *Quaternary Science Reviews*, 226, 105998,
540 <https://doi.org/10.1016/j.quascirev.2019.105998>, 2019.
- 541 Band, S., Yadava, M. G., Lone, M. A., Shen, C. C., Sree, K., and Ramesh, R.: High-resolution mid-Holocene
542 Indian Summer Monsoon recorded in a stalagmite from the Kotumsar Cave, Central India, *Quaternary
543 International*, 479, 19-24, <https://doi.org/10.1016/j.quaint.2018.01.026>, 2018.
- 544 Bar-Matthews, M., Ayalon, A., Gilmour, M., Matthews, A., and Hawkesworth, C. J.: Sea-land oxygen
545 isotopic relationships from planktonic foraminifera and speleothems in the Eastern Mediterranean region
546 and their implication for paleorainfall during interglacial intervals, *Geochimica et Cosmochimica Acta*, 67,
547 3181-3199, [https://doi.org/10.1016/S0016-7037\(02\)01031-1](https://doi.org/10.1016/S0016-7037(02)01031-1), 2003.
- 548 Blaauw, M.: Methods and code for ‘classical’ age-modelling of radiocarbon sequences, *Quaternary
549 Geochronology*, 5, 512-518, <https://doi.org/10.1016/j.quageo.2010.01.002>, 2010.
- 550 Blaauw, M., and Christen, J. A.: Flexible Paleoclimate Age-Depth Models Using an Autoregressive Gamma
551 Process, *Bayesian Analysis*, 6, 457-474, <https://doi.org/10.1214/11-ba618>, 2011.
- 552 Braun, K., Nehme, C., Pickering, R., Rogerson, M., and Scropton, N.: A Window into Africa’s Past
553 Hydroclimates: The SISAL_v1 Database Contribution, *Quaternary*, 2,
554 <https://doi.org/10.3390/quat2010004>, 2019a.
- 555 Braun, K., Bar-Matthews, M., Matthews, A., Ayalon, A., Cowling, R. M., Karkanas, P., Fisher, E. C., Dyez, K.,
556 Zilberman, T., and Marean, C. W.: Late Pleistocene records of speleothem stable isotopic compositions
557 from Pinnacle Point on the South African south coast, *Quaternary Research*, 91, 265-288,
558 <https://doi.org/10.1017/qua.2018.61>, 2019b.
- 559 Breitenbach, S. F. M., Rehfeld, K., Goswami, B., Baldini, J. U. L., Ridley, H. E., Kennett, D. J., Prufer, K. M.,
560 Aquino, V. V., Asmerom, Y., Polyak, V. J., Cheng, H., Kurths, J., and Marwan, N.: COConstructing Proxy Records
561 from Age models (COPRA), *Climate of the Past*, 8, 1765-1779, <https://doi.org/10.5194/cp-8-1765-2012>,
562 2012.
- 563 Breitenbach, S. F. M., Plessen, B., Waltgenbach, S., Tjallingii, R., Leonhardt, J., Jochum, K. P., Meyer, H.,
564 Goswami, B., Marwan, N., and Scholz, D.: Holocene interaction of maritime and continental climate in
565 Central Europe: New speleothem evidence from Central Germany, *Global and Planetary Change*, 176, 144-
566 161, <https://doi.org/10.1016/J.GLOPLACHA.2019.03.007>, 2019.
- 567 Bronk Ramsey, C.: Deposition models for chronological records, *Quaternary Science Reviews*, 27, 42-60,
568 ~~2008~~<https://doi.org/10.1016/j.quascirev.2007.01.019>, 2008.
- 569 Bronk Ramsey, C.: Bayesian analysis of radiocarbon dates, *Radiocarbon*, 51, 337-360, ~~2009~~;
570 <https://doi.org/10.1017/S0033822200033865>, 2009.
- 571 Bronk Ramsey, C., and Lee, S.: Recent and planned developments of the program OxCal, *Radiocarbon*, 55,
572 720-730, ~~2013~~https://doi.org/10.2458/azu_js_rc.55.16215, 2013.
- 573 Budsky, A., Scholz, D., Wassenburg, J. A., Mertz-Kraus, R., Spötl, C., Riechelmann, D. F. C., Gibert, L.,
574 Jochum, K. P., and Andraea, M. O.: Speleothem $\delta^{13}\text{C}$ record suggests enhanced spring/summer drought

- 575 in south-eastern Spain between 9.7 and 7.8 ka – A circum-Western Mediterranean anomaly?, *The*
 576 *Holocene*, 29, 1113-1133, <https://doi.org/10.1177/0959683619838021>, 2019.
- 577 Burns, S. J., Fleitmann, D., Matter, A., Kramers, J., and Al-Subbary, A. A.: Indian Ocean Climate and an
 578 Absolute Chronology over Dansgaard/Oeschger Events 9 to 13, *Science*, 301, 1365-1367,
 579 <https://doi.org/10.1126/science.1086227>, 2003.
- 580 Burns, S. J., Fleitmann, D., Matter, A., Kramers, J., and Al-Subbary, A. A.: Corrections and Clarifications,
 581 *Science*, 305, 1567a-1567a, <https://doi.org/10.1126/science.305.5690.1567a>, 2004.
- 582 Burns, S. J., Welsh, L. K., Scroxton, N., Cheng, H., and Edwards, R. L.: Millennial and orbital scale variability
 583 of the South American Monsoon during the penultimate glacial period, *Scientific Reports*, 9, 1234,
 584 <https://doi.org/10.1038/s41598-018-37854-3>, 2019.
- 585 Burstyn, Y., Martrat, B., Lopez, F. J., Iriarte, E., Jacobson, J. M., Lone, A. M., and Deininger, M.: Speleothems
 586 from the Middle East: An Example of Water Limited Environments in the SISAL Database, *Quaternary*, 2,
 587 <https://doi.org/10.3390/quat2020016>, 2019.
- 588 Cai, Y. J., Chiang, J. C. H., Breitenbach, S. F. M., Tan, L. C., Cheng, H., Edwards, R. L., and An, Z. S.: Holocene
 589 moisture changes in western China, Central Asia, inferred from stalagmites, *Quaternary Science Reviews*,
 590 158, 15-28, <https://doi.org/10.1016/j.quascirev.2016.12.014>, 2017.
- 591 Carolin, S. A., Cobb, K. M., Lynch-Stieglitz, J., Moerman, J. W., Partin, J. W., Lejau, S., Malang, J., Clark, B.,
 592 Tuen, A. A., and Adkins, J. F.: Northern Borneo stalagmite records reveal West Pacific hydroclimate across
 593 MIS 5 and 6, *Earth and Planetary Science Letters*, 439, 182-193,
 594 <https://doi.org/10.1016/j.epsl.2016.01.028>, 2016.
- 595 Carolin, S. A., Walker, R. T., Day, C. C., Ersek, V., Sloan, R. A., Dee, M. W., Talebian, M., and Henderson, G.
 596 M.: Precise timing of abrupt increase in dust activity in the Middle East coincident with 4.2 ka social
 597 change, *Proceedings of the National Academy of Sciences*, 116, 67-72,
 598 <https://doi.org/10.1073/PNAS.1808103115>, 2019.
- 599 ~~Chen, Z., Auler, A. S., Bakalowicz, M., Drew, D., Griger, F., Hartmann, J., Jiang, G., Moosdorf, N., Richts, A.,~~
 600 ~~Stevanovic, Z., Veni, G., and Goldscheider, N.: The World Karst Aquifer Mapping project: concept, mapping~~
 601 ~~procedure and map of Europe, *Hydrogeology Journal*, 25, 771-785, [10.1007/s10040-016-1519-3](https://doi.org/10.1007/s10040-016-1519-3), 2017.~~
- 602 Cheng, H., Edwards, R. L., Wan, Y. J., Ko, X. G., Ming, Y. F., Kelly, M. J., Wang, X. F., Gallup, C. D., and Liu,
 603 W. G.: A penultimate glacial monsoon record from Hulu Cave and two-phase glacial terminations, *Geology*,
 604 34, 217-220, <https://doi.org/10.1130/g22289.1>, 2006.
- 605 Cheng, H., Fleitmann, D., Edwards, R. L., Wang, X., Cruz, F. W., Auler, A. S., Mangini, A., Wang, Y., Kong, X.,
 606 Burns, S. J., and Matter, A.: Timing and structure of the 8.2 kyr B.P. event inferred from $\delta^{18}O$ records of
 607 stalagmites from China, Oman, and Brazil, *Geology*, 37, 1007-1010, <https://doi.org/10.1130/G30126A.1>,
 608 2009.
- 609 Cheng, H., Sinha, A., Cruz, F. W., Wang, X., Edwards, R. L., d'Horta, F. M., Ribas, C. C., Vuille, M., Stott, L.
 610 D., and Auler, A. S.: Climate change patterns in Amazonia and biodiversity, *Nature Communications*, 4,
 611 1411, <https://doi.org/10.1038/ncomms2415>, 2013.
- 612 Cheng, H., Springer, G. S., Sinha, A., Hardt, B. F., Yi, L., Li, H., Tian, Y., Li, X., Rowe, H. D., Kathayat, G., Ning,
 613 Y., and Edwards, R. L.: Eastern North American climate in phase with fall insolation throughout the last
 614 three glacial-interglacial cycles, *Earth and Planetary Science Letters*, 522, 125-134,
 615 <https://doi.org/10.1016/j.epsl.2019.06.029>, 2019.

- 616 Columbu, A., Spötl, C., De Waele, J., Yu, T.-L., Shen, C.-C., and Gázquez, F.: A long record of MIS 7 and MIS
617 5 climate and environment from a western Mediterranean speleothem (SW Sardinia, Italy), *Quaternary*
618 *Science Reviews*, 220, 230-243, <https://doi.org/10.1016/J.QUASCIREV.2019.07.023>, 2019.
- 619 Comas-Bru, L., and Harrison, S. P.: SISAL: Bringing added value to speleothem research, *Quaternary*, 2, 7,
620 <https://doi.org/10.3390/quat2010007>, 2019.
- 621 Comas-Bru, L., Harrison, S. P., Werner, M., Rehfeld, K., Scropton, N., Veiga-Pires, C., and SISAL Working
622 Group members: Evaluating model outputs using integrated global speleothem records of climate change
623 since the last glacial, *Climate of the Past*, 15, 1557-1579, <https://doi.org/10.5194/cp-15-1557-2019>, 2019.
- 624 Comas-Bru, L., Atsawawaranunt, K., Harrison, S.P. and SISAL Working Group members: SISAL (Speleothem
625 Isotopes Synthesis and AnaLysis Working Group) database version 2.0. University of Reading. Dataset.
626 http://dx.doi.org/10.17864/1947.242_2020https://doi.org/10.17864/1947.256_2020a.
- 627 [Comas-Bru, L., Deininger, M., Fohlmeister, J., Baker, A., McDermott, F., and Scholz, D.: Quality control of](https://doi.org/10.5281/zenodo.3631443)
628 [the dating information table in the SISAL database. Zenodo. http://doi.org/10.5281/zenodo.3631443,](https://doi.org/10.5281/zenodo.3631443)
629 [2020b.](https://doi.org/10.5281/zenodo.3631443)
- 630 Cruz, F. W., Burns, S. J., Karmann, I., Sharp, W. D., and Vuille, M.: Reconstruction of regional atmospheric
631 circulation features during the late Pleistocene in subtropical Brazil from oxygen isotope composition of
632 speleothems, *Earth and Planetary Science Letters*, 248, 495-507,
633 <https://doi.org/10.1016/J.EPSL.2006.06.019>, 2006.
- 634 Czuppon, G., Demeny, A., Leel-Ossy, S., Ovari, M., Molnar, M., Stieber, J., Kiss, K., Karman, K., Suranyi, G.,
635 and Haszpra, L.: Cave monitoring in the Beke and Baradla caves (Northeastern Hungary): implications for
636 the conditions for the formation cave carbonates, *International Journal of Speleology*, 47, 13-28,
637 <https://doi.org/10.5038/1827-806x.47.1.2110>, 2018.
- 638 Deininger, M., Ward, M. B., Novello, F. V., and Cruz, W. F.: Late Quaternary Variations in the South
639 American Monsoon System as Inferred by Speleothems—New Perspectives Using the SISAL Database,
640 *Quaternary*, 2, <https://doi.org/10.3390/quat2010006>, 2019.
- 641 Demény, A., Kern, Z., Németh, A., Frisia, S., Hatvani, I. G., Czuppon, G., Leél-Őssy, S., Molnár, M., Óvári,
642 M., Surányi, G., Gilli, A., Wu, C.-C., and Shen, C.-C.: North Atlantic influences on climate conditions in East-
643 Central Europe in the late Holocene reflected by flowstone compositions, *Quaternary International*, 512,
644 99-112, <https://doi.org/10.1016/J.QUAINT.2019.02.014>, 2019.
- 645 Denniston, R. F., Asmerom, Y., Lachniet, M., Polyak, V. J., Hope, P., An, N., Rodzinyak, K., and Humphreys,
646 W. F.: A Last Glacial Maximum through middle Holocene stalagmite record of coastal Western Australia
647 climate, *Quaternary Science Reviews*, 77, 101-112, <https://doi.org/10.1016/j.quascirev.2013.07.002>,
648 2013a.
- 649 Denniston, R. F., Wyrwoll, K.-H., Polyak, V. J., Brown, J. R., Asmerom, Y., Wanamaker, A. D., LaPointe, Z.,
650 Ellerbroek, R., Barthelmes, M., Cleary, D., Cugley, J., Woods, D., and Humphreys, W. F.: A Stalagmite record
651 of Holocene Indonesian–Australian summer monsoon variability from the Australian tropics, *Quaternary*
652 *Science Reviews*, 78, 155-168, <https://doi.org/10.1016/J.QUASCIREV.2013.08.004>, 2013b.
- 653 Denniston, R. F., Asmerom, Y., Polyak, V. J., Wanamaker, A. D., Ummenhofer, C. C., Humphreys, W. F.,
654 Cugley, J., Woods, D., and Lucker, S.: Decoupling of monsoon activity across the northern and southern
655 Indo-Pacific during the Late Glacial, *Quaternary Science Reviews*, 176, 101-105,
656 <https://doi.org/10.1016/J.QUASCIREV.2017.09.014>, 2017a.

- 657 Denniston, R. F., Houts, A. N., Asmerom, Y., Wanamaker, A. D., Haws, J. A., Polyak, V. J., Thatcher, D. L.,
658 Altan-Ochir, S., Borowske, A. C., Breitenbach, S. F. M., Ummenhofer, C. C., Regala, F. T., Benedetti, M. M.,
659 and Bicho, N.: A Stalagmite Test of North Atlantic SST and Iberian Hydroclimate Linkages over the Last
660 Two Glacial Cycles, *Climate of the Past Discussions*, 14, 1893-1913, <https://doi.org/10.5194/cp-2017-146>,
661 2017b.
- 662 Dong, J., Shen, C.-C., Kong, X., Wu, C.-C., Hu, H.-M., Ren, H., and Wang, Y.: Rapid retreat of the East Asian
663 summer monsoon in the middle Holocene and a millennial weak monsoon interval at 9 ka in northern
664 China, *Journal of Asian Earth Sciences*, 151, 31-39, <https://doi.org/10.1016/J.JSEAES.2017.10.016>, 2018.
- 665 Dumitru, O. A., Onac, B. P., Polyak, V. J., Wynn, J. G., Asmerom, Y., and Fornos, J. J.: Climate variability in
666 the western Mediterranean between 121 and 67 ka derived from a Mallorcan speleothem record,
667 *Palaeogeography Palaeoclimatology Palaeoecology*, 506, 128-138,
668 <https://doi.org/10.1016/j.palaeo.2018.06.028>, 2018.
- 669 El-Shenawy, M. I., Kim, S. T., Schwarcz, H. P., Asmerom, Y., and Polyak, V. J.: Speleothem evidence for the
670 greening of the Sahara and its implications for the early human dispersal out of sub-Saharan Africa,
671 *Quaternary Science Reviews*, 188, 67-76, <https://doi.org/10.1016/j.quascirev.2018.03.016>, 2018.
- 672 Fleitmann, D., Cheng, H., Badertscher, S., Edwards, R. L., Mudelsee, M., Göktürk, O. M., Fankhauser, A.,
673 Pickering, R., Raible, C. C., Matter, A., Kramers, J., and Tüysüz, O.: Timing and climatic impact of Greenland
674 interstadials recorded in stalagmites from northern Turkey, *Geophysical Research Letters*, 36, L19707-
675 L19707, <https://doi.org/10.1029/2009GL040050>, 2009.
- 676 Flohr, P., Fleitmann, D., Zorita, E., Sadekov, A., Cheng, H., Bosomworth, M., Edwards, L., Matthews, W.,
677 and Matthews, R.: Late Holocene droughts in the Fertile Crescent recorded in a speleothem from northern
678 Iraq, *Geophysical Research Letters*, 44, 1528-1536, <https://doi.org/10.1002/2016GL071786>, 2017.
- 679 Frappier, A., Sahagian, D., González, L. A., and Carpenter, S. J.: El Nino Events Recorded by Stalagmite
680 Carbon Isotopes, *Science*, 298, 565-565, <https://doi.org/10.1126/science.1076446>, 2002.
- 681 Frappier, A. B., Sahagian, D., Carpenter, S. J., Gonzalez, L. A., and Frappier, B. R.: Stalagmite stable isotope
682 record of recent tropical cyclone events, *Geology*, 35, 111-114, <https://doi.org/10.1130/g23145a.1>, 2007.
- 683 Gautam, P. K., Narayana, A. C., Band, S. T., Yadava, M. G., Ramesh, R., Wu, C.-C., and Shen, C.-C.: High-
684 resolution reconstruction of Indian summer monsoon during the Bølling-Allerød from a central Indian
685 stalagmite, *Palaeogeography, Palaeoclimatology, Palaeoecology*, 514, 567-576,
686 <https://doi.org/10.1016/J.PALAEO.2018.11.006>, 2019.
- 687 Göktürk, O. M., Fleitmann, D., Badertscher, S., Cheng, H., Edwards, R. L., Leuenberger, M., Fankhauser, A.,
688 Tüysüz, O., and Kramers, J.: Climate on the southern Black Sea coast during the Holocene: implications
689 from the Sofular Cave record, *Quaternary Science Reviews*, 30, 2433-2445,
690 <https://doi.org/10.1016/J.QUASCIREV.2011.05.007>, 2011.
- 691 [Goldscheider, N., Chen, Z., Auler, A. S., Bakalowicz, M., Broda, S., Drew, D., Hartmann, J., Jiang, G.,
692 Moosdorf, N., Stevanovic, Z., and Veni, G.: Global distribution of carbonate rocks and karst water
693 resources, *Hydrogeology Journal*, 28, 1661-1677, <https://doi.org/10.1007/s10040-020-02139-5>, 2020.](https://doi.org/10.1007/s10040-020-02139-5)
- 694 Haslett, J., and Parnell, A.: A simple monotone process with application to radiocarbon-dated depth
695 chronologies, *Journal of the Royal Statistical Society: Series C (Applied Statistics)*, 57, 399-418,
696 [2008:https://doi.org/10.1111/j.1467-9876.2008.00623.x](https://doi.org/10.1111/j.1467-9876.2008.00623.x), 2008.

- 697 Hu, J, Emile-Geay J., and Partin J.: Correlation-based interpretations of paleoclimate data—where statistics
698 meet past climates. *Earth and Planetary Science Letters* 459, 362-371,
699 [2017-https://doi.org/10.1016/j.epsl.2016.11.048](https://doi.org/10.1016/j.epsl.2016.11.048), 2017.
- 700 Huguet, C., Routh, J., Fietz, S., Lone, M. A., Kalpana, M. S., Ghosh, P., Mangini, A., Kumar, V., and
701 Rangarajan, R.: Temperature and Monsoon Tango in a Tropical Stalagmite: Last Glacial-Interglacial Climate
702 Dynamics, *Scientific Reports*, 8, 5386, <https://doi.org/10.1038/s41598-018-23606-w>, 2018.
- 703 Isola, I., Zanchetta, G., Drysdale, R. N., Regattieri, E., Bini, M., Bajo, P., Hellstrom, J. C., Baneschi, I., Lionello,
704 P., Woodhead, J., and Greig, A.: The 4.2 ka event in the central Mediterranean: New data from a Corchia
705 speleothem (Apuan Alps, central Italy), *Climate of the Past*, 15, 135-151, <https://doi.org/10.5194/cp-15-135-2019>, 2019.
- 707 Jamieson, R. A., Baldini, J. U. L., Frappier, A. B., and Müller, W.: Volcanic ash fall events identified using
708 principal component analysis of a high-resolution speleothem trace element dataset, *Earth and Planetary
709 Science Letters*, 426, 36-45, <https://doi.org/10.1016/J.EPSL.2015.06.014>, 2015.
- 710 Jex, C. N., Baker, A., Fairchild, I. J., Eastwood, W. J., Leng, M. J., Sloane, H. J., Thomas, L., and Bekaroglu,
711 E.: Calibration of speleothem delta O-18 with instrumental climate records from Turkey, *Global and
712 Planetary Change*, 71, 207-217, <https://doi.org/10.1016/j.gloplacha.2009.08.004>, 2010.
- 713 Jex, C. N., Baker, A., Eden, J. M., Eastwood, W. J., Fairchild, I. J., Leng, M. J., Thomas, L., and Sloane, H. J.:
714 A 500 yr speleothem-derived reconstruction of late autumn-winter precipitation, northeast Turkey,
715 *Quaternary Research*, 75, 399-405, <https://doi.org/10.1016/j.yqres.2011.01.005>, 2011.
- 716 Jex, C. N., Phipps, S. J., Baker, A., and Bradley, C.: Reducing uncertainty in the climatic interpretations of
717 speleothem delta O-18, *Geophysical Research Letters*, 40, 2259-2264, <https://doi.org/10.1002/grl.50467>,
718 2013.
- 719 Jiang, X., He, Y., Shen, C., Kong, X., Li, Z., and Chang, Y.: Stalagmite-inferred Holocene precipitation in
720 northern Guizhou Province, China, and asynchronous termination of the Climatic Optimum in the Asian
721 monsoon territory, *Chinese Science Bulletin*, 57, 795-801, <https://doi.org/10.1007/s11434-011-4848-6>,
722 2012.
- 723 Jiang, X., He, Y., Shen, C.-C., Li, Z., and Lin, K.: Replicated stalagmite-inferred centennial-to decadal-scale
724 monsoon precipitation variability in southwest China since the mid Holocene, *The Holocene*, 23, 841-849,
725 <https://doi.org/10.1177/0959683612471986>, 2013.
- 726 Jo, K.-n., Yi, S., Lee, J.-Y., Woo, K. S., Cheng, H., Edwards, L. R., and Kim, S.-T.: 1000-Year Quasi-Periodicity
727 of Weak Monsoon Events in Temperate Northeast Asia since the Mid-Holocene, *Scientific Reports*, 7,
728 15196, <https://doi.org/10.1038/s41598-017-15566-4>, 2017.
- 729 Johnson, K. R., Ingram, B. L., Sharp, W. D., and Zhang, P. Z.: East Asian summer monsoon variability during
730 Marine Isotope Stage 5 based on speleothem $\delta^{18}\text{O}$ records from Wanxiang Cave, central China,
731 *Palaeogeography Palaeoclimatology Palaeoecology*, 236, 5-19,
732 <https://doi.org/10.1016/j.palaeo.2005.11.041>, 2006.
- 733 Kanner, L. C., Burns, S. J., Cheng, H., and Edwards, R. L.: High-Latitude Forcing of the South American
734 Summer Monsoon During the Last Glacial, *Science*, 335, 570-573,
735 <https://doi.org/10.1126/science.1213397>, 2012.
- 736 Kanner, L. C., Burns, S. J., Cheng, H., Edwards, R. L., and Vuille, M.: High-resolution variability of the South
737 American summer monsoon over the last seven millennia: insights from a speleothem record from the

- 738 central Peruvian Andes, Quaternary Science Reviews, 75, 1-10,
739 <https://doi.org/10.1016/j.quascirev.2013.05.008>, 2013.
- 740 Kathayat, G., Cheng, H., Sinha, A., Yi, L., Li, X. L., Zhang, H. W., Li, H. Y., Ning, Y. F., and Edwards, R. L.: The
741 Indian monsoon variability and civilization changes in the Indian subcontinent, Science Advances, 3,
742 e1701296, <https://doi.org/10.1126/sciadv.1701296>, 2017.
- 743 Kathayat, G., Cheng, H., Sinha, A., Berkelhammer, M., Zhang, H., Duan, P., Li, H., Li, X., Ning, Y., and
744 Edwards, R. L.: Evaluating the timing and structure of the 4.2 ka event in the Indian summer monsoon
745 domain from an annually resolved speleothem record from Northeast India, Climate of the Past, 14, 1869-
746 1879, <https://doi.org/10.5194/cp-14-1869-2018>, 2018.
- 747 Kaushal, N., Breitenbach, F. M. S., Lechleitner, A. F., Sinha, A., Tewari, C. V., Ahmad, M. S., Berkelhammer,
748 M., Band, S., Yadava, M., Ramesh, R., and Henderson, M. G.: The Indian Summer Monsoon from a
749 Speleothem $\delta^{18}\text{O}$ Perspective—A Review, Quaternary, 1, 29, <https://doi.org/10.3390/quat1030029>,
750 2018.
- 751 Kern, Z., Demény, A., Perşoiu, A., and Hatvani, G. I.: Speleothem Records from the Eastern Part of Europe
752 and Turkey—Discussion on Stable Oxygen and Carbon Isotopes, Quaternary, 2,
753 <https://doi.org/10.3390/quat2030031>, 2019.
- 754 Krause, C. E., Gagan, M. K., Dunbar, G. B., Hantoro, W. S., Hellstrom, J. C., Cheng, H., Edwards, R. L.,
755 Suwargadi, B. W., Abram, N. J., and Rifai, H.: Spatio-temporal evolution of Australasian monsoon
756 hydroclimate over the last 40,000 years, Earth and Planetary Science Letters, 513, 103-112,
757 <https://doi.org/10.1016/J.EPSL.2019.01.045>, 2019.
- 758 Lachniet, M. S., Asmerom, Y., Burns, S. J., Patterson, W. P., Polyak, V. J., and Seltzer, G. O.: Tropical
759 response to the 8200 yr BP cold event? Speleothem isotopes indicate a weakened early Holocene
760 monsoon in Costa Rica, Geology, 32, 957-960, <https://doi.org/10.1130/g20797.1>, 2004.
- 761 Lachniet, M. S., Johnson, L., Asmerom, Y., Burns, S. J., Polyak, V., Patterson, W. P., Burt, L., and Azouz, A.:
762 Late Quaternary moisture export across Central America and to Greenland: evidence for tropical rainfall
763 variability from Costa Rican stalagmites, Quaternary Science Reviews, 28, 3348-3360,
764 <https://doi.org/10.1016/J.QUASCIREV.2009.09.018>, 2009.
- 765 Laskar, A. H., Yadava, M. G., Ramesh, R., Polyak, V. J., and Asmerom, Y.: A 4 kyr stalagmite oxygen isotopic
766 record of the past Indian Summer Monsoon in the Andaman Islands, Geochemistry, Geophysics,
767 Geosystems, 14, 3555-3566, <https://doi.org/10.1002/ggge.20203>, 2013.
- 768 Lauritzen, S.-E., and Onac, B. P.: Isotopic Stratigraphy of a Last Interglacial Stalagmite from Northwestern
769 Romania: Correlation with the Deep-Sea record and Northern-Latitude Speleothem, Journal of Cave and
770 Karst Studies, 61, 22-30, 1999.
- 771 Lechleitner, F. A., Amirnezhad-Mozhdehi, S., Columbu, A., Comas-Bru, L., Labuhn, I., Pérez-Mejías, C., and
772 Rehfeld, K.: The Potential of Speleothems from Western Europe as Recorders of Regional Climate: A
773 Critical Assessment of the SISAL Database, Quaternary, 1, <https://doi.org/10.3390/quat1030030>, 2018.
- 774 Li, H., Cheng, H., Sinha, A., Kathayat, G., Spötl, C., André, A. A., Meunier, A., Biswas, J., Duan, P., Ning, Y.,
775 and Edwards, R. L.: Hydro-climatic variability in the southwestern Indian Ocean between 6000 and 3000
776 years ago, Climate of the Past, 14, 1881-1891, <https://doi.org/10.5194/cp-14-1881-2018>, 2018.
- 777 Liu, X., Rao, Z., Shen, C. C., Liu, J., Chen, J., Chen, S., Wang, X., and Chen, F.: Holocene Solar Activity Imprint
778 on Centennial- to Multidecadal-Scale Hydroclimatic Oscillations in Arid Central Asia, Journal of
779 Geophysical Research: Atmospheres, 124, 2562-2573, <https://doi.org/10.1029/2018JD029699>, 2019.

- 780 Logan, A. J.: A new paleoclimate record for North Westland, New Zealand, with implications for the
781 interpretation of speleothem based paleoclimate proxies, Master of Science, Geology, University of
782 Canterbury, 109 pp., 2011. <http://hdl.handle.net/10092/5762>
- 783 Lončar, N., Bar-Matthews, M., Ayalon, A., Faivre, S., and Surić, M.: Holocene climatic conditions in the
784 eastern Adriatic recorded in stalagmites from Strašna peć Cave (Croatia), *Quaternary International*, 508,
785 98-106, <https://doi.org/10.1016/j.quaint.2018.11.006>, 2019.
- 786 Lorrey, A., Williams, P., Salinger, J., Martin, T., Palmer, J., Fowler, A., Zhao, J.-x., and Neil, H.: Speleothem
787 stable isotope records interpreted within a multi-proxy framework and implications for New Zealand
788 palaeoclimate reconstruction, *Quaternary International*, 187, 52-75,
789 <https://doi.org/10.1016/j.quaint.2007.09.039>, 2008.
- 790 Marsh, A., Fleitmann, D., Al-Manmi, D. A. M., Altaweel, M., Wengrow, D., and Carter, R.: Mid- to late-
791 Holocene archaeology, environment and climate in the northeast Kurdistan region of Iraq, *The Holocene*,
792 28, 955-967, <https://doi.org/10.1177/0959683617752843>, 2018.
- 793 McCabe-Glynn, S., Johnson, K. R., Strong, C., Berkelhammer, M., Sinha, A., Cheng, H., and Edwards, R. L.:
794 Variable North Pacific influence on drought in southwestern North America since AD 854, *Nature*
795 *Geoscience*, 6, 617-621, <https://doi.org/10.1038/ngeo1862>, 2013.
- 796 Medina-Elizalde, M., Burns, S. J., Polanco-Martinez, J. M., Beach, T., Lases-Hernandez, F., Shen, C. C., and
797 Wang, H. C.: High-resolution speleothem record of precipitation from the Yucatan Peninsula spanning the
798 Maya Preclassic Period, *Global and Planetary Change*, 138, 93-102,
799 <https://doi.org/10.1016/j.gloplacha.2015.10.003>, 2016.
- 800 Medina-Elizalde, M., Burns, S. J., Polanco-Martinez, J., Lases-Hernandez, F., Bradley, R., Wang, H. C., and
801 Shen, C. C.: Synchronous precipitation reduction in the American Tropics associated with Heinrich 2,
802 *Scientific Reports*, 7, <https://doi.org/10.1038/s41598-017-11742-8>, 2017.
- 803 Moseley, G. E., Spötl, C., Brandstätter, S., Erhardt, T., Luetscher, M., and Edwards, R. L.: NALPS19: Sub-
804 orbital scale climate variability recorded in Northern Alpine speleothems during the last glacial period,
805 *Climate of the Past*, 16, 29-50, <https://doi.org/10.5194/cp-16-19-2020>, 2020.
- 806 Mudelsee, M., Fohlmeister, J. and Scholz, D.: Effects of dating errors on nonparametric trend analyses of
807 speleothem time series, *Climate of the Past*, 8, 1637-1648, <https://doi.org/10.5194/cp-8-1637-2012>,
808 2012.
- 809 Niggemann, S., Mangini, A., Mudelsee, M., Richter, D. K., and Wurth, G.: Sub-Milankovitch climatic cycles
810 in Holocene stalagmites from Sauerland, Germany, *Earth and Planetary Science Letters*, 216, 539-547,
811 [https://doi.org/10.1016/S0012-821X\(03\)00513-2](https://doi.org/10.1016/S0012-821X(03)00513-2), 2003a.
- 812 Niggemann, S., Mangini, A., Richter, D. K., and Wurth, G.: A paleoclimate record of the last 17,600 years
813 in stalagmites from the B7 cave, Sauerland, Germany, *Quaternary Science Reviews*, 22, 555-567,
814 [https://doi.org/10.1016/S0277-3791\(02\)00143-9](https://doi.org/10.1016/S0277-3791(02)00143-9), 2003b.
- 815 Osete, M. L., Martin-Chivelet, J., Rossi, C., Edwards, R. L., Egli, R., Munoz-Garcia, M. B., Wang, X. F., Pavon-
816 Carrasco, F. J., and Heller, F.: The Blake geomagnetic excursion recorded in a radiometrically dated
817 speleothem, *Earth and Planetary Science Letters*, 353, 173-181,
818 <https://doi.org/10.1016/j.epsl.2012.07.041>, 2012.
- 819 Oster, J. L., Warken, S. F., Sekhon, N., Arienzo, M., and Lachniet, M.: Speleothem Paleoclimatology for the
820 Caribbean, Central America, and North America, *Quaternary*, 2, <https://doi.org/10.3390/quat2010005>,
821 2019.

- 822 Parnell, A.: Bchron: Radiocarbon dating, age-depth modelling, relative sea level rate estimation, and non-
823 parametric phase modelling, R package version 4.3.0., 2018.
- 824 Partin, J. W., Quinn, T. M., Shen, C. C., Okumura, Y., Cardenas, M. B., Siringan, F. P., Banner, J. L., Lin, K.,
825 Hu, H. M., and Taylor, F. W.: Gradual onset and recovery of the Younger Dryas abrupt climate event in the
826 tropics, *Nature Communications*, 6, 8061-8061, <https://doi.org/10.1038/ncomms9061>, 2015.
- 827 Pawlak, J., Błaszczak, M., Hercman, H., and Matoušková, Š.: A continuous stable isotope record of last
828 interglacial age from the Bulgarian Cave Orlova Chuka, *Geochronometria*, 46, 87-101,
829 <https://doi.org/10.1515/geochr-2015-0107>, 2019.
- 830 Peckover, E. N., Andrews, J. E., Leeder, M. R., Rowe, P. J., Marca, A., Sahy, D., Noble, S., and Gawthorpe,
831 R.: Coupled stalagmite – Alluvial fan response to the 8.2 ka event and early Holocene palaeoclimate
832 change in Greece, *Palaeogeography, Palaeoclimatology, Palaeoecology*, 532, 109252-109252,
833 <https://doi.org/10.1016/j.palaeo.2019.109252>, 2019.
- 834 Polyak, V. J., Asmerom, Y., and Lachniet, M. S.: Rapid speleothem $\delta^{13}\text{C}$ change in southwestern North
835 America coincident with Greenland stadial 20 and the Toba (Indonesia) supereruption, *Geology*, 45, 843-
836 846, <https://doi.org/10.1130/g39149.1>, 2017.
- 837 R Core Team: R: A language and environment for statistical computing. R Foundation for Statistical
838 Computing, Vienna, Austria, <http://www.r-project.org/index.html>, 2019.
- 839 Rehfeld, K., and Kurths, J.: Similarity estimators for irregular and age-uncertain time series, *Climate of the*
840 *Past*, 10, 107-122, 2014. <https://doi.org/10.5194/cp-10-107-2014>, 2014.
- 841 [Rehfeld, K., Goswami B., Juncu, D. Marwan N. and Breitenbach, S.: COPRA – Constructing Proxy Records](https://doi.org/10.5194/cp-10-107-2014)
842 [From Age Models. https://tocsy.pik-potsdam.de/copra.php](https://tocsy.pik-potsdam.de/copra.php) Version 1.15, last mod. 02-Nov-2017, 2017.
- 843 [Rehfeld, K., Roesch, C., Comas-Bru, L., and Amirnezhad-Mozhdehi, S.: Age-depth model ensembles for](https://doi.org/10.5281/zenodo.3816804)
844 [SISAL v2 speleothem records \(Version 1.0\) \[Data set\]. Zenodo. http://doi.org/10.5281/zenodo.3816804,](https://doi.org/10.5281/zenodo.3816804)
845 [2020.](https://doi.org/10.5281/zenodo.3816804)
- 846 Rivera-Collazo, I., Winter, A., Scholz, D., Mangini, A., Miller, T., Kushnir, Y., and Black, D.: Human
847 adaptation strategies to abrupt climate change in Puerto Rico ca. 3.5 ka, *Holocene*, 25, 627-640,
848 <https://doi.org/10.1177/0959683614565951>, 2015.
- 849 Roesch, C., and Rehfeld, K.: Automatising construction and evaluation of age-depth models for hundreds
850 of speleothems, 9th International Workshop on Climate Informatics, 2019.
- 851 Rossi, C., Mertz-Kraus, R., and Osete, M. L.: Paleoclimate variability during the Blake geomagnetic
852 excursion (MIS 5d) deduced from a speleothem record, *Quaternary Science Reviews*, 102, 166-180,
853 <https://doi.org/10.1016/j.quascirev.2014.08.007>, 2014.
- 854 Rossi, C., Bajo, P., Lozano, R. P., and Hellstrom, J.: Younger Dryas to Early Holocene paleoclimate in
855 Cantabria (N Spain): Constraints from speleothem Mg, annual fluorescence banding and stable isotope
856 records, *Quaternary Science Reviews*, 192, 71-85, <https://doi.org/10.1016/j.quascirev.2018.05.025>, 2018.
- 857 Rudzka-Phillips, D., McDermott, F., Jackson, A., and Fleitmann, D.: Inverse modelling of the C-14 bomb
858 pulse in stalagmites to constrain the dynamics of soil carbon cycling at selected European cave sites,
859 *Geochimica et Cosmochimica Acta*, 112, 32-51, <https://doi.org/10.1016/j.gca.2013.02.032>, 2013.

- 860 Rudzka, D., McDermott, F., and Suric, M.: A late Holocene climate record in stalagmites from Modric Cave
861 (Croatia), *Journal of Quaternary Science*, 27, 585-596, <https://doi.org/10.1002/jqs.2550>, 2012.
- 862 Scholz, D., and Hoffmann, D. L.: StalAge - An algorithm designed for construction of speleothem age
863 models, *Quaternary Geochronology*, 6, 369-382, <https://doi.org/10.1016/j.quageo.2011.02.002>, 2011.
- 864 Scroxton, N., Burns, S. J., McGee, D., Hardt, B., Godfrey, L. R., Ranivoharimanana, L., and Faina, P.:
865 Competing Temperature and Atmospheric Circulation Effects on Southwest Madagascan Rainfall During
866 the Last Deglaciation, *Paleoceanography and Paleoclimatology*, 34, 275-286,
867 <https://doi.org/10.1029/2018PA003466>, 2019.
- 868 Sinha, N., Gandhi, N., Chakraborty, S., Krishnan, R., Yadava, M. G., and Ramesh, R.: Abrupt climate change
869 at ~2800 yr BP evidenced by a stalagmite record from peninsular India, *The Holocene*, 28, 1720-1730,
870 <https://doi.org/10.1177/0959683618788647>, 2018.
- 871 Staubwasser, M., Drăgușin, V., Onac, B. P., Assonov, S., Ersek, V., Hoffmann, D. L., and Veres, D.: Impact
872 of climate change on the transition of Neanderthals to modern humans in Europe, *Proceedings of the
873 National Academy of Sciences of the United States of America*, 115, 9116-9121,
874 <https://doi.org/10.1073/pnas.1808647115>, 2018.
- 875 Steponaitis, E., Andrews, A., McGee, D., Quade, J., Hsieh, Y. T., Broecker, W. S., Shuman, B. N., Burns, S. J.,
876 and Cheng, H.: Mid-Holocene drying of the US Great Basin recorded in Nevada speleothems, *Quaternary
877 Science Reviews*, 127, 174-185, <https://doi.org/10.1016/j.quascirev.2015.04.011>, 2015.
- 878 Strikis, N. M., Chiessi, C. M., Cruz, F. W., Vuille, M., Cheng, H., Barreto, E. A. D., Mollenhauer, G., Kasten,
879 S., Karmann, I., Edwards, R. L., Bernal, J. P., and Sales, H. D.: Timing and structure of Mega-SACZ events
880 during Heinrich Stadial 1, *Geophysical Research Letters*, 42, 5477-5484,
881 <https://doi.org/10.1002/2015gl064048>, 2015.
- 882 Strikis, N. M., Cruz, F. W., Barreto, E. A. S., Naughton, F., Vuille, M., Cheng, H., Voelker, A. H. L., Zhang, H.,
883 Karmann, I., Edwards, R. L., Auler, A. S., Santos, R. V., and Sales, H. R.: South American monsoon response
884 to iceberg discharge in the North Atlantic, *Proceedings of the National Academy of Sciences of the United
885 States of America*, 115, 3788-3793, <https://doi.org/10.1073/pnas.1717784115>, 2018.
- 886 Talma, A. S. and Vogel, J. C.: Late Quaternary Paleotemperatures Derived from a Speleothem from Cango
887 Caves, Cape Province, South Africa, *Quaternary Research*, 37(2), 203-213, [https://doi.org/10.1016/0033-
888 5894\(92\)90082-t](https://doi.org/10.1016/0033-5894(92)90082-t), 1992.
- 889 Tan, L., An, Z., Huh, C.-A., Cai, Y., Shen, C.-C., Shiao, L.-J., Yan, L., Cheng, H., and Edwards, R. L.: Cyclic
890 precipitation variation on the western Loess Plateau of China during the past four centuries, *Scientific
891 Reports*, 4, 6381-6381, <https://doi.org/10.1038/srep06381>, 2015.
- 892 Tan, L., Cai, Y., Cheng, H., Edwards, L. R., Gao, Y., Xu, H., Zhang, H., and An, Z.: Centennial- to decadal-scale
893 monsoon precipitation variations in the upper Hanjiang River region, China over the past 6650 years, *Earth
894 and Planetary Science Letters*, 482, 580-590, <https://doi.org/10.1016/j.epsl.2017.11.044>, 2018a.
- 895 Tan, L., Cai, Y., Cheng, H., Edwards, L. R., Lan, J., Zhang, H., Li, D., Ma, L., Zhao, P., and Gao, Y.: High
896 resolution monsoon precipitation changes on southeastern Tibetan Plateau over the past 2300 years,
897 *Quaternary Science Reviews*, 195, 122-132, <https://doi.org/10.1016/J.QUASCIREV.2018.07.021>, 2018b.
- 898 Tzedakis, P. C., Drysdale, R. N., Margari, V., Skinner, L. C., Menviel, L., Rhodes, R. H., Taschetto, A. S.,
899 Hodell, D. A., Crowhurst, S. J., Hellstrom, J. C., Fallick, A. E., Grimalt, J. O., McManus, J. F., Martrat, B.,

- 900 Mokeddem, Z., Parrenin, F., Regattieri, E., Roe, K., and Zanchetta, G.: Enhanced climate instability in the
901 North Atlantic and southern Europe during the Last Interglacial, *Nature Communications*, 9, 4235-4235,
902 <https://doi.org/10.1038/s41467-018-06683-3>, 2018.
- 903 van Breukelen, M. R., Vonhof, H. B., Hellstrom, J. C., Wester, W. C. G., and Kroon, D.: Fossil dripwater in
904 stalagmites reveals Holocene temperature and rainfall variation in Amazonia, *Earth and Planetary Science*
905 *Letters*, 275, 54-60, <https://doi.org/10.1016/J.EPSL.2008.07.060>, 2008.
- 906 Van Rangelbergh, M., Fleitmann, D., Verheyden, S., Cheng, H., Edwards, L., De Geest, P., De
907 Vleeschouwer, D., Burns, S. J., Matter, A., Claeys, P., and Keppens, E.: Mid- to late Holocene Indian Ocean
908 Monsoon variability recorded in four speleothems from Socotra Island, Yemen, *Quaternary Science*
909 *Reviews*, 65, 129-142, <https://doi.org/10.1016/j.quascirev.2013.01.016>, 2013.
- 910 Verheyden, S., Keppens, E., Fairchild, I. J., McDermott, F., and Weis, D.: Mg, Sr and Sr isotope geochemistry
911 of a Belgian Holocene speleothem: implications for paleoclimate reconstructions, *Chemical Geology*, 169,
912 131-144, [https://doi.org/10.1016/S0009-2541\(00\)00299-0](https://doi.org/10.1016/S0009-2541(00)00299-0), 2000.
- 913 Verheyden, S., Keppens, E., Quinif, Y., Cheng, H. J., and Edwards, L. R.: Late-glacial and Holocene climate
914 reconstruction as inferred from a stalagmite-Grotte du Père Noël, Han-sur-Lesse, Belgium, *Geologica*
915 *Belgica*, 17, 83-89, <https://popups.uliege.be:443/1374-8505/index.php?id=4421&file=1&pid=4412>, 2014.
- 916 Wang, J. K., Johnson, K. R., Borsato, A., Amaya, D. J., Griffiths, M. L., Henderson, G. M., Frisia, S., and
917 Mason, A.: Hydroclimatic variability in Southeast Asia over the past two millennia, *Earth and Planetary*
918 *Science Letters*, 525, 115737-115737, <https://doi.org/10.1016/j.epsl.2019.115737>, 2019.
- 919 Wang, Y. J., Cheng, H., Edwards, R. L., Kong, X. G., Shao, X. H., Chen, S. T., Wu, J. Y., Jiang, X. Y., Wang, X.
920 F., and An, Z. S.: Millennial- and orbital-scale changes in the East Asian monsoon over the past 224,000
921 years, *Nature*, 451, 1090-1093, <https://doi.org/10.1038/nature06692>, 2008.
- 922 Ward, B. M., Wong, C. I., Novello, V. F., McGee, D., Santos, R. V., Silva, L. C. R., Cruz, F. W., Wang, X.,
923 Edwards, R. L., and Cheng, H.: Reconstruction of Holocene coupling between the South American
924 Monsoon System and local moisture variability from speleothem $\delta^{18}\text{O}$ and $^{87}\text{Sr}/^{86}\text{Sr}$ records, *Quaternary*
925 *Science Reviews*, 210, 51-63, <https://doi.org/10.1016/J.QUASCIREV.2019.02.019>, 2019.
- 926 Warken, S. F., Fohlmeister, J., Schröder-Ritzrau, A., Constantin, S., Spötl, C., Gerdes, A., Esper, J., Frank, N.,
927 Arps, J., Terente, M., Riechelmann, D. F. C., Mangini, A. and Scholz, D.: Reconstruction of late Holocene
928 autumn/winter precipitation variability in SW Romania from a high-resolution speleothem trace element
929 record, *Earth Planet. Sci. Lett.*, 499, 122–133, <https://doi.org/10.1016/j.epsl.2018.07.027>, 2018.
- 930 Warken, S. F., Scholz, D., Spötl, C., Jochum, K. P., Pajón, J. M., Bahr, A., and Mangini, A.: Caribbean
931 hydroclimate and vegetation history across the last glacial period, *Quaternary Science Reviews*, 218, 75-
932 90, <https://doi.org/10.1016/J.QUASCIREV.2019.06.019>, 2019.
- 933 Webb, M., Dredge, J., Barker, P. A., Muller, W., Jex, C., Desmarchelier, J., Hellstrom, J., and Wynn, P. M.:
934 Quaternary climatic instability in south-east Australia from a multi-proxy speleothem record, *Journal of*
935 *Quaternary Science*, 29, 589-596, <https://doi.org/10.1002/jqs.2734>, 2014.
- 936 Weber, M., Scholz, D., Schröder-Ritzrau, A., Deininger, M., Spötl, C., Lugli, F., Mertz-Kraus, R., Jochum, K.
937 P., Fohlmeister, J., Stumpf, C. F., and Riechelmann, D. F. C.: Evidence of warm and humid interstadials in
938 central Europe during early MIS 3 revealed by a multi-proxy speleothem record, *Quaternary Science*
939 *Reviews*, 200, 276-286, <https://doi.org/10.1016/J.QUASCIREV.2018.09.045>, 2018.

- 940 Wendt, K. A., Häuselmann, A. D., Fleitmann, D., Berry, A. E., Wang, X., Auler, A. S., Cheng, H., and Edwards,
941 R. L.: Three-phased Heinrich Stadial 4 recorded in NE Brazil stalagmites, *Earth and Planetary Science*
942 *Letters*, 510, 94-102, <https://doi.org/10.1016/J.EPSL.2018.12.025>, 2019.
- 943 Whittaker, T. E.: High-resolution speleothem-based palaeoclimate records from New Zealand reveal
944 robust teleconnection to North Atlantic during MIS 1-4, Unpubl. PhD Thesis, The University of Waikato,
945 2008.
- 946 Wilcox, P. S., Dorale, J. A., Baichtal, J. F., Spötl, C., Fowell, S. J., Edwards, R. L., and Kovarik, J. L.: Millennial-
947 scale glacial climate variability in Southeastern Alaska follows Dansgaard-Oeschger cyclicality, *Scientific*
948 *Reports*, 9, 7880-7880, <https://doi.org/10.1038/s41598-019-44231-1>, 2019.
- 949 Williams, P. W., King, D. N. T., Zhao, J. X., and Collerson, K. D.: Late pleistocene to holocene composite
950 speleothem O-18 and C-13 chronologies from south island, new Zealand-did a global younger dryas really
951 exist?, *Earth and Planetary Science Letters*, 230, 301-317, <https://doi.org/10.1016/j.epsl.2004.10.024>,
952 2005.
- 953 Williams, P. W., Neil, H. L., and Zhao, J. X.: Age frequency distribution and revised stable isotope curves
954 for New Zealand speleothems: palaeoclimatic implications, *International Journal of Speleology*, 39, 99-
955 112, <https://doi.org/10.5038/1827-806x.39.2.5>, 2010.
- 956 Wu, J. Y., Wang, Y. J., Cheng, H., Kong, X. G., and Liu, D. B.: Stable isotope and trace element investigation
957 of two contemporaneous annually-laminated stalagmites from northeastern China surrounding the 8.2 ka
958 event, *Climate of the Past*, 8, 1497-1507, <https://doi.org/10.5194/cp-8-1497-2012>, 2012.
- 959 Yadava, M. G., Ramesh, R., and Pant, G. B.: Past monsoon rainfall variations in peninsular India recorded
960 in a 331-year-old speleothem, *Holocene*, 14, 517-524, <https://doi.org/10.1191/0959683604hl728rp>,
961 2004.
- 962 Yin, J. J., Li, H. C., Rao, Z. G., Shen, C. C., Mii, H. S., Pillutla, R. K., Hu, H. M., Li, Y. X., and Feng, X. H.:
963 Variations of monsoonal rain and vegetation during the past millennium in Tianguai Mountain, North China
964 reflected by stalagmite delta O-18 and delta C-13 records from Zhenzhu Cave, *Quaternary International*,
965 447, 89-101, <https://doi.org/10.1016/j.quaint.2017.06.039>, 2017.
- 966 Zhang, H., Cheng, H., Cai, Y., Spötl, C., Kathayat, G., Sinha, A., Edwards, R. L., and Tan, L.: Hydroclimatic
967 variations in southeastern China during the 4.2 ka event reflected by stalagmite records, *Climate of the*
968 *Past*, 14, 1805-1817, <https://doi.org/10.5194/cp-14-1805-2018>, 2018a.
- 969 Zhang, H., Cheng, H., Spötl, C., Cai, Y., Sinha, A., Tan, L., Yi, L., Yan, H., Kathayat, G., Ning, Y., Li, X., Zhang,
970 F., Zhao, J., and Edwards, R. L.: A 200-year annually laminated stalagmite record of precipitation
971 seasonality in southeastern China and its linkages to ENSO and PDO, *Scientific Reports*, 8, 12344-12344,
972 <https://doi.org/10.1038/s41598-018-30112-6>, 2018b.
- 973 Zhang, H., Ait Brahim, Y., Li, H., Zhao, J., Kathayat, G., Tian, Y., Baker, J., Wang, J., Zhang, F., Ning, Y.,
974 Edwards, L. R., and Cheng, H.: The Asian Summer Monsoon: Teleconnections and Forcing Mechanisms—
975 A Review from Chinese Speleothem $\delta^{18}\text{O}$ Records, *Quaternary*, 2, <https://doi.org/10.3390/quat2030026>,
976 2019.
- 977 Zhang, H. B., Griffiths, M. L., Huang, J. H., Cai, Y. J., Wang, C. F., Zhang, F., Cheng, H., Ning, Y. F., Hu, C. Y.,
978 and Xie, S. C.: Antarctic link with East Asian summer monsoon variability during the Heinrich Stadial-Bølling
979 interstadial transition, *Earth and Planetary Science Letters*, 453, 243-251,
980 <https://doi.org/10.1016/j.epsl.2016.08.008>, 2016.

- 981 Zhang, H. L., Yu, K. F., Zhao, J. X., Feng, Y. X., Lin, Y. S., Zhou, W., and Liu, G. H.: East Asian Summer Monsoon
982 variations in the past 12.5 ka: High-resolution delta O-18 record from a precisely dated aragonite
983 stalagmite in central China, *Journal of Asian Earth Sciences*, 73, 162-175,
984 <https://doi.org/10.1016/j.jseaes.2013.04.015>, 2013.
- 985 Zhang, P., Cheng, H., Edwards, R. L., Chen, F., Wang, Y., Yang, X., Liu, J., Tan, M., Wang, X., Liu, J., An, C.,
986 Dai, Z., Zhou, J., Zhang, D., Jia, J., Jin, L., and Johnson, K. R.: A Test of Climate, Sun, and Culture Relationships
987 from an 1810-Year Chinese Cave Record, *Science*, 322, 940-942,
988 <https://doi.org/10.1126/science.1163965>, 2008.